

1

Version dated: November 6, 2019

2 RH: Phylogenetic biome shifts among paleobiomes

3

Modeling phylogenetic biome shifts on a planet with a past

5 MICHAEL J. LANDIS^{1,2,*}, ERIKA J. EDWARDS², AND MICHAEL J. DONOGHUE²

6 *¹Department of Biology, Washington University in St. Louis, Rebstock Hall, St. Louis, Missouri,
7 63130, USA*

8 *²Department of Ecology & Evolutionary Biology, Environmental Sciences Center, Yale University,
9 New Haven, Connecticut, 06511, USA*

10 *Corresponding author: Michael J. Landis, Department of Biology, Washington
11 University in St. Louis, Rebstock Hall, St. Louis, Missouri, 63130, USA; E-mail:
12 michael.landis@wustl.edu.

13 *Abstract.*—The spatial distribution of biomes has changed considerably over deep time, so
14 the geographical opportunity for an evolutionary lineage to shift into a new biome depends
15 on how the availability and connectivity of biomes has varied temporally. To better
16 understand how lineages shift between biomes in space and time, we developed a
17 phylogenetic biome shift model in which each lineage shifts between biomes and disperses
18 between regions at rates that depend on the lineage's biome affinity and location relative to
19 the spatiotemporal distribution of biomes at any given time. To study the behavior of the
20 biome shift model in an empirical setting, we developed a literature-based representation of
21 paleobiome structure for three mesic forest biomes, six regions, and eight time strata,
22 ranging from the Late Cretaceous (100 Ma) through the present. We then fitted the model
23 to a time-calibrated phylogeny of 119 *Viburnum* species to compare how the results
24 responded to various realistic or unrealistic assumptions about paleobiome structure.
25 Ancestral biome estimates that account for paleobiome dynamics reconstructed a warm
26 temperate (or tropical) origin of *Viburnum*, which is consistent with previous fossil-based
27 estimates of ancestral biomes. In *Viburnum*, imposing unrealistic paleobiome distributions
28 led to ancestral biome estimates that eliminated support for tropical origins, and instead
29 inflated support for cold temperate ancestry during the warmer Paleocene and Eocene. The
30 biome shift model we describe is applicable to the study of evolutionary systems beyond
31 *Viburnum*, and the core mechanisms of our model are extensible to the design of richer
32 phylogenetic models of historical biogeography and/or lineage diversification. We conclude
33 that biome shift models that account for dynamic geographical opportunities are important
34 for inferring ancestral biomes that are compatible with our understanding of Earth history.
35 (Keywords: phylogenetics, ancestral states, biome shifts, niche conservatism, historical
36 biogeography)

37

INTRODUCTION

38 Biomes are ecologically and climatically distinct species assemblages that vary in size,
39 shape, and continuity across geographical regions, in large part due to regional differences
40 in temperature, seasonality, altitude, soil types, and continentality (Whittaker 1970; Wolfe
41 1985; Olson et al. 2001; Mucina 2019). The diversity of biomes occupied by particular
42 lineages also varies considerably, with some clades exhibiting strict associations with
43 particular biomes, and others showing multiple transitions between biomes over time
44 (Donoghue and Edwards 2014). Although it is accepted that cladewide variation in
45 regional biome occupancy was generated and is maintained by evolutionary forces including
46 speciation, extinction, dispersal, and adaptation to new biomes, it remains difficult to
47 estimate exactly when, where, and under what conditions phylogenetic lineages first shifted
48 into the biomes that their descendants inhabit today.

49 In current practice, ancestral regions and biome affinities are often estimated
50 independently of one another, and then relationships between regions and biomes are
51 compared post hoc (Crisp et al. 2009; Weeks et al. 2014). Although such studies yield
52 important evolutionary insights, the estimates themselves do not account for how lineages
53 might move between regions or adapt to newly encountered biomes given the temporally
54 variable spatial configuration of biomes across regions. Conceptually, the regional
55 availability of a biome should influence how easily a lineage might disperse into a new
56 region or shift into a new biome, an effect Donoghue and Edwards (2014) termed
57 geographical opportunity. One strategy to model this effect first defines discrete regions
58 that are exactly coincident with modern day biomes, and then assumes that species within
59 a given region occur within the corresponding biome. Cardillo et al. (2017) carried out
60 such an analysis in studying the biogeography of the Australian plant clade, *Hakea*
61 (Proteaceae), using method features developed by Matzke (2014), where total regional area
62 and shared perimeter lengths tuned dispersal rates between regions. This innovative
63 strategy depends crucially on the uniformity of biome composition within each region.

64 Larger, discrete regions may very well be dominated by a single biome type, yet still be
65 composed of assorted dominant, subdominant, and marginal biome types at local scales.

66 More importantly for our purposes, defining geographical opportunity based on
67 modern biome features (such as area and shared perimeter), may be problematic in
68 instances where the spatial distribution of biomes has changed considerably over time,
69 since those changes should also influence when and where ancestral lineages shift between
70 regions and biomes. For example, if woodlands dominated a particular region until the rise
71 of grasslands, that might inform when a grassland-adapted lineage first dispersed into that
72 region. That is, if the presence or absence of biomes in regions influences modern species
73 ranges, then temporal variation in regional biome availability should influence our models
74 of range evolution.

75 To model how paleoecological dynamics might influence range evolution, Meseguer
76 et al. (2015) fitted ecological niche models (ENMs) to fossil data so as to limit the
77 connectivity between regions for models that estimate ancestral ranges (Ree and Smith
78 2008). While this strategy is quite promising, its current form requires that the clade under
79 study (*Hypericum* of Hypericaceae, in their case) has a sufficiently rich fossil record over
80 space and time to inform the ENM. It also assumes that all lineages face the same, broad
81 ecological limitations to range evolution, independent of what particular biome affinity
82 each lineage possesses at a given moment. Although the quality of the fossil record is
83 largely out of our control, the second assumption could be relaxed: ideally, if a clade
84 contains sub-lineages that specialize in woodland or in grassland habitats, any particular
85 lineages range should be principally limited by the availability of the specific biome to
86 which that lineage is adapted, rather than being constrained based on a broader,
87 clade-wide average of grassland and woodland lineages.

88 In this paper, we aim to address the aforementioned challenges facing current
89 phylogenetic models of biome shifting by incorporating four key properties: (1) that biome
90 shifts and dispersal events share a common state space over biomes and regions, (2) that

91 discrete regions may contain a number of different biomes, (3) that the geographical
92 structure of biomes within and between regions can vary over time, and (4) that lineages
93 adapted to different biomes and located in different regions will experience different
94 dispersal rates between regions and different shift rates into new biomes. We begin by
95 introducing a graph-based approach to characterize the availability, prevalence, and
96 connectivity of regional biomes through time, building on the framework introduced by
97 Landis (2017). We then develop an event-based evolutionary process using a time-stratified
98 continuous-time Markov chain that models biome shifts and dispersal given the ways in
99 which biome distributions have changed over time. Because the exact influence of extrinsic
100 geographical factors and/or ecological structure is bound to vary from clade to clade, the
101 degree of influence of such features on the evolutionary model are treated as free
102 parameters to be estimated from the data itself.

103 To explore the possible importance of paleobiome structure on lineage movements
104 among biomes, we apply our model to *Viburnum*, a genus of 165 species that originated in
105 the Late Cretaceous and are today found in tropical, warm temperate, and cold temperate
106 forests throughout Eurasia and the New World. We generated paleobiome graphs for these
107 three mesic forest biomes across six continental regions for eight major epochs over the
108 past hundred million years. Fitting the model to our *Viburnum* dataset all-but-eliminates
109 the possibility of a cold temperate origin of the clade. This is consistent with our
110 understanding of the important biogeographic role of the boreotropics during the Paleocene
111 and Eocene, and with our recent fossil-based ancestral biome estimates in *Viburnum*
112 (Landis et al. 2019).

113

METHODS

114

Viburnum phylogeny and biogeography

115 *Viburnum* (Adoxaceae) is a clade of about 163 extant plant species that originated
116 just before the Cretaceous-Paleogene (K-Pg) boundary, roughly 70 Ma. Previous studies of
117 phylogenetic relationships (Clement et al. 2014; Spriggs et al. 2015; Eaton et al. 2017) and
118 divergence times (Spriggs et al. 2015; Landis et al. 2019) provide a firm basis for
119 understanding the order and timing of lineage diversification events in *Viburnum*. In this
120 study, we focus on a subsample of 119 *Viburnum* species with relationships that are highly
121 supported by phylogenomic data (Eaton et al. 2017; Landis et al. 2019) and whose
122 divergence times were time-calibrated under the fossilized-birth death process (Heath et al.
123 2014) as described in (Landis et al. 2019).

124 *Viburnum* is found in six continental-scale regions: Southeast Asia, including the
125 Indoaustralian Archipelago and the Indian subcontinent; East Asia, including China,
126 Taiwan, and Japan; Europe, including the North African coast, portions of the Middle
127 East, and the Azores and the Canary Islands; a North American region north of Mexico; a
128 Central American region that includes Mexico, Cuba, and Jamaica; and in the South
129 American Andes. Across those regions, living viburnums are affiliated with mesic forest
130 biomes and show widespread parallel evolution of leaf form, leafing habit, and physiology
131 coincident with transitions between warmer and colder biomes (Schmerler et al. 2012;
132 Chatelet et al. 2013; Spriggs et al. 2015; Scoffoni et al. 2016; Edwards et al. 2017). Five
133 extinct *Viburnum* lineages are known by their fossil pollen grains recovered from North
134 American and European locales. Four of these are older samples (48 to 33 Ma) from
135 paleofloral communities that we previously judged to be warm temperate or subtropical
136 (Landis et al. 2019). For our analyses in this study, we defined three mesic forest biomes
137 based on annual temperatures and rainfall patterns (Edwards et al. 2017). Tropical forests
138 have high temperatures and precipitation year round, showing little seasonality. Warm
139 temperate forests, which include paratropical, lucidophyllous, and cloud forests, vary
140 seasonally in temperature and precipitation, but do not experience prolonged freezing
141 temperatures during the coldest months. Cold temperate forests also experience seasonal

142 temperatures and precipitation, but average minimum temperatures drop below freezing in
143 at least one of the coldest months.

144 Because we are interested in how biome states and regional states evolve in tandem,
145 we constructed a set of $3 \times 6 = 18$ compound states that we call biome-region states.

146 Throughout the paper, we identify the biome-region state for a lineage in biome state i and
147 region state k with the notation (i,k) . However, in practice, we encode biome-region states
148 as integers with values from 1 to 18. Biome-region state codings for *Viburnum* are
149 translated from Landis et al. (2019), though here we combine cloud forests and warm
150 temperate forests into a single warm temperate category. Ambiguous biome states (for
151 several warm or cold temperate East Asian species) were recoded as ambiguous for the
152 relevant biome-region states. The time-calibrated phylogeny and the updated biome-region
153 character matrix for *Viburnum* are hosted on DataDryad (LINK).

154 *Model overview*

155 Our aim is to model a regional biome shift process that allows changes in the
156 spatiotemporal distribution of biomes to influence the likelihood of a lineage shifting
157 between biomes and dispersing between regions. This process can be described in terms of
158 interactions between two fundamental subprocesses: the biome shift process and the
159 dispersal process.

160 The biome shift process models when and where lineages shift into new biome types.
161 The probability of a biome shift clearly depends on intrinsic and extrinsic factors governing
162 how readily a lineage might adapt to the conditions in a new biome, a myriad of factors
163 that we do not fully explore here. Rather, we focus specifically on modeling the effect of
164 geographical opportunity on biome shifts (Donoghue and Edwards 2014). For example, it is
165 plausible that a species inhabiting the warm temperate forests of Europe might shifted into
166 the tropical biome during the Early Eocene, a period when tropical rain forests could be
167 found at latitudes as extreme as 60° N. In contrast, a biome shift within Europe from a

168 warm temperate to a tropical biome would be less likely today or during any time after the
169 global cooling trend that began with the Oligocene.

170 The dispersal process models how lineages move between regions. The rate of
171 dispersal between regions should depend on how connected those regions are for a given
172 biome affinity. Returning to the Europe example, a tropical lineage in Southeast Asia
173 might have a relatively high dispersal rate into Europe during the Early Eocene, when
174 Europe was predominantly tropical and warm temperate, as compared to today, when
175 Europe is dominated by temperate and boreal forests.

176 Figure 1 depicts the basic behavior of the biome shift and dispersal processes in
177 response to an evolving biome structure. By characterizing known features of paleobiome
178 structure (Fig. 1A) into adjacency matrices (Fig. 1B), we can differentiate between
179 probable and improbable phylogenetic histories of biome shifts and dispersal events (Fig.
180 1C) based on time-dependent and paleobiome-informed biome shift rates (Fig. 1D) and
181 dispersal rates (Fig. 1E). Of the two regional biome shift histories in Figure 1C, the first
182 history invokes three events that are fully congruent with the underlying paleobiome
183 structure. The second history requires only two events, yet those events are incongruent
184 with the paleobiome structure. But which regional biome shift history is more probable?
185 Assigning probabilities to histories must depend not only on the phylogenetic placement
186 and age of the regional biome shift events, but also on the degree to which the clade
187 evolves in a paleobiome-dependent manner. We later return to how this unknown behavior
188 of the evolutionary process may be estimated from phylogenetic data.

189 *An evolving spatial distribution of biomes through time*

190 Biome availability and connectivity has evolved over time. We summarize these
191 dynamics with a series of time-dependent graphs that are informed by the paleobiological
192 and paleogeographical literature (Figure 2). To define our paleobiome graphs, we consulted
193 global biome reconstructions generated by Wolfe (1985), Morley (2000), Graham (2011,

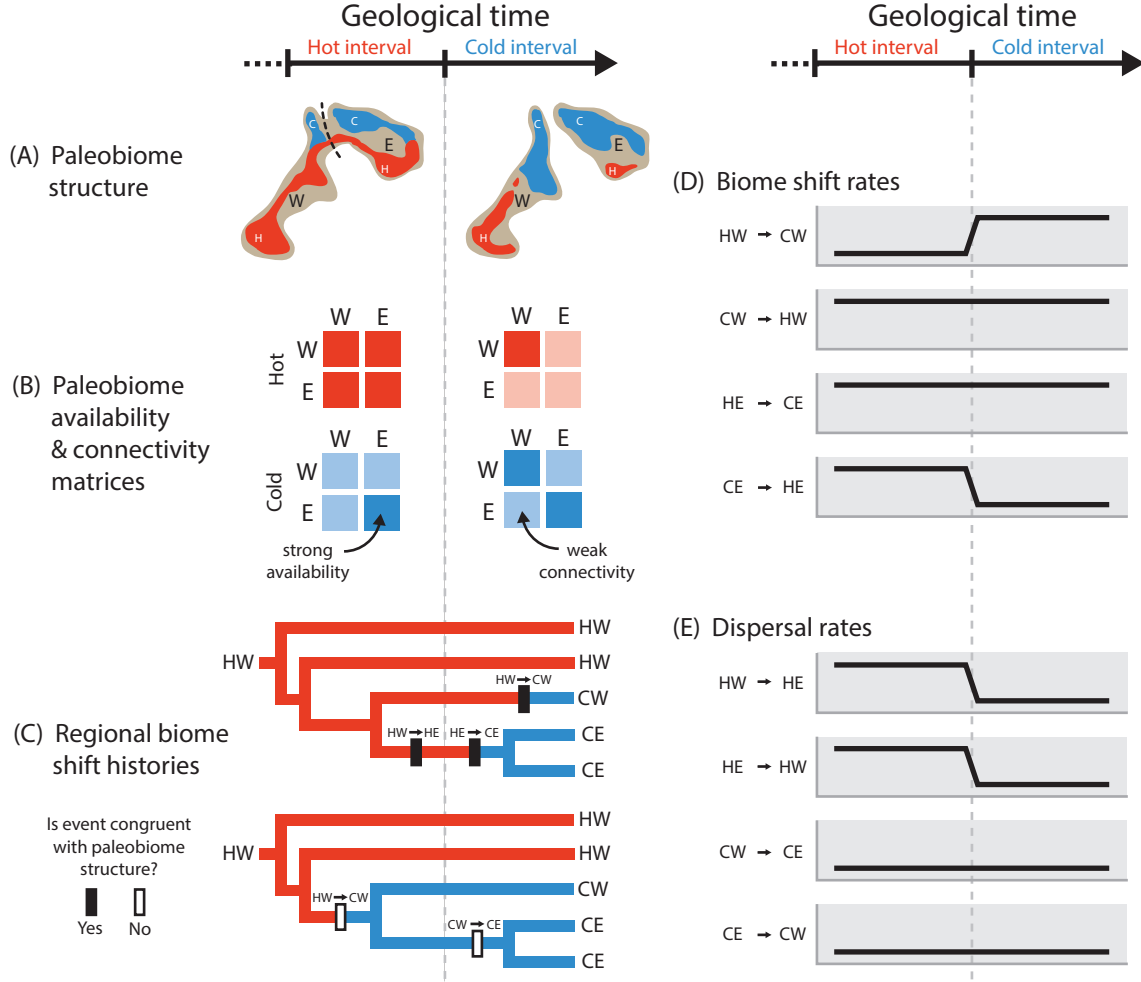


Figure 1: Cartoon of the relationship between paleobiome structure and a regional biome shift process. The left and right panels are aligned to the same geological time scale that is divided into a Hot (red) interval followed by a Cold (blue) interval. (A) Maps of paleobiome structure with two regions, East (E) and West (W), and two focal biomes of interest, Hot (H) and Cold (C), in which the expansive Hot biome is replaced by the Cold biome as the East and West regions separate. (B) Paleobiome adjacency matrices encode the availability of biomes within regions and the connectivity of biomes between regions based on whether paleobiome features are strong (dark) or weak (light). Diagonal elements reflect biome availability within regions while off-diagonal elements report biome connectivity between regions. (C) Two possible regional biome shift histories for a phylogeny with a western, hot-adapted (HW) origin. Lineages shift between biomes at rates that depend on the availability of biomes within the lineage's current region and disperse between regions at rates that depend on connectivity of the lineage's current biome between regions. The two histories require (top) or do not require (bottom) evolutionary events to be congruent with paleobiome structure. (D) Time-dependent biome shift rates for the four possible events: HW to CW, CW to HW, HE to CE, and CE to HE. (E) Time-dependent dispersal rates for the four possible events: HW to HE, HE to HW, CW to CE, and CE to CW.

194 2018), Fine and Ree (2006), Jetz and Fine (2012), and Willis and McElwain (2014) which
195 we then corroborated with biome reconstructions quantitatively estimated using the
196 BIOME4 model (Prentice et al. 1992; Kaplan et al. 2003) for times corresponding to the
197 Early-Mid Eocene (Herold et al. 2014), the Late Ecoene and the Oligocene (Pound and
198 Salzmann 2017), the Mid-Late Miocene (Pound et al. 2011, 2012), and the Pliocene
199 (Salzmann et al. 2008, 2009). For epochs that lack published BIOME4 reconstructions, we
200 compared our paleobiome maps to reconstructions built from proprietary data kindly
201 provided by P. J. Valdes (pers. comm.).

202 We classified the availability and connectivity of biomes within regions into three
203 categories—dominant, subdominant, and marginal—that were appropriate to the scale of
204 the regions and the precision of the ancestral biome estimates. Dominant biomes, with a
205 strong presence, displayed $\geq 25\%$ regional coverage, subdominant biomes with a weak
206 presence covered $< 25\%$ of a region, while biomes with marginal presence covered $< 1\%$ of a
207 region. Likewise, the connectivity of a biome between two regions at a given time is scored
208 as either strong, weak, or marginal, depending on how continuously biomes are inferred to
209 have been distributed near regional adjacencies. Independent of the distribution of biomes,
210 we similarly scored the geographical connectivity between regions as strong, weak, and
211 marginal, using the equivalent of the modern connection between Central and South
212 America through the Isthmus as Panama to minimally qualify as strong connectivity, and
213 distances between modern Europe and North America to represent weak connectivity.
214 Together, the availability and connectivity for each region, each biome, and each timeslice
215 is encoded into a series of paleobiome graphs, which we later use to define the rates at
216 which biome shift and dispersal events occur.

217 Our paleobiome graphs capture several important aspects of how mesic forest
218 biomes moved and evolved (Fig. 2). The Late Cretaceous through the Paleocene and Early
219 Eocene was a prolonged period of warm, wet conditions during which the poles had little to
220 no ice. Throughout that time, tropical forests were dominant in all six of our regions, while

221 warm temperate forests dominated only throughout East Asia, Europe, and North
222 America. Together, the tropical and warm temperate forests formed a beltway of
223 boreotropical forests around the northern hemisphere (Wolfe 1985; Morley 2000; Willis and
224 McElwain 2014; Graham 2011, 2018), that persisted through the Mid/Late Eocene. With
225 the Oligocene, the opening of the Drake Passage and the closure of the Tethys Sea
226 redirected global ocean currents. Together with steep declines in atmospheric CO₂ levels,
227 this ushered in cooler and drier conditions worldwide. This global climatic change
228 progressively restricted tropical forests to more equatorial regions, inducing the disjunction
229 we find among modern tropical forests (Latham and Ricklefs 1993; Wiens and Donoghue
230 2004; Donoghue 2008). As the boreotropical forests receded, they were first replaced by
231 warm temperate forests, and then eventually by cold temperate and boreal forests.
232 Following this global revolution of biome structure, connectivity between Old World and
233 New World tropical forests never again matched that of the Paleocene-Eocene
234 boreotropical beltway. Our paleobiome graphs are designed to be simple, but not too
235 simplistic to study how phylogenetic biome shift models respond to a geographical biome
236 structure that evolves with time.

237 Figure 2 helps illustrate how a lineage might evolve with respect to different
238 distributions of biomes within and between regions over time. A lineage that freely
239 disperses between regions and shifts between biomes regardless of the historical condition
240 of the planet might transition between regions under fully connected matrices (Null, first
241 column). Lineages that are only dispersal-limited by terrestrial connectivity disperse under
242 the adjacency constraints encoded in the second column of matrices (Geographical, second
243 column). However, lineages that are dispersal-limited by biome availability and
244 connectivity might disperse according to the paleobiome patterns shown in the third, fourth
245 and fifth columns (tropical, T; warm temperate, W; and cold temperate, C). For example,
246 a lineage that is strictly adapted to the warm temperate biome would disperse according to
247 the warm temperate series of paleobiome graphs (fourth column). If that lineage shifted its

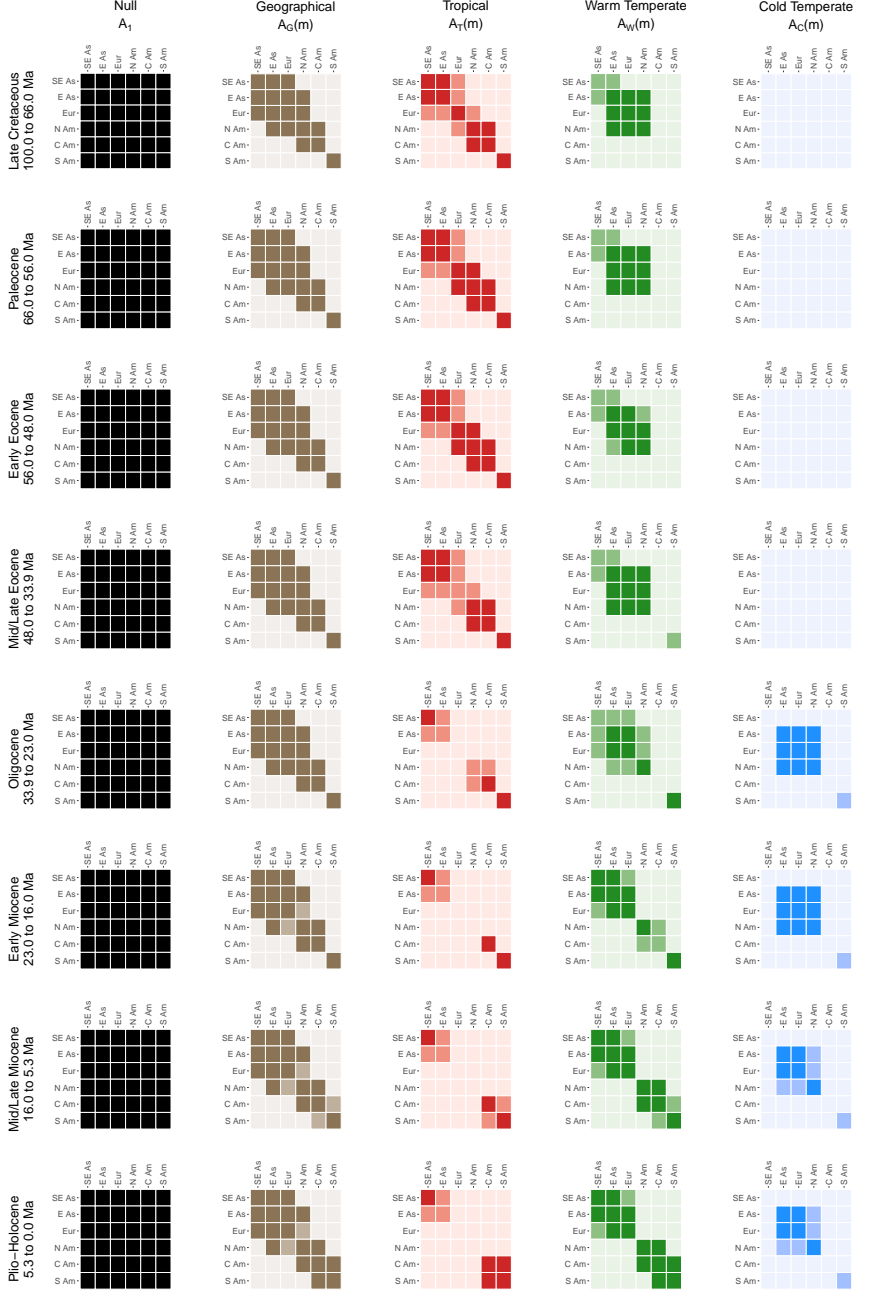


Figure 2: Availability and connectivity of biomes from Late Cretaceous (100 Ma) to Present. Adjacency matrices are used as empirical priors to shape the time-stratified phylogenetic biome shift process. Rows correspond to eight time intervals, while columns correspond to regional features, specifically full (or null) connectivity (black), simple geographical connectivity (brown), or features involving the tropical (red), warm temperate (green), and cold temperate (blue) forest biomes. The matrix for each time and feature encodes the availability of (the diagonal) and the connectivity between (off-diagonal) regions for that feature at that time, where matrix rows and columns correspond to source and destination regions, respectively. Availability/connectivity is marked as being strong (dark), weak (medium), or marginal (light).

248 affinity from a warm temperate to a tropical biome, that lineage would thereafter shift
249 between biomes and disperse between regions under the adjacency matrix structures of the
250 tropical biome (third column) until the lineage next shifted biomes. However, biome shift
251 rates also should depend on what biomes are locally accessible. For example, a North
252 American lineage would have the geographical opportunity to shift from warm temperate
253 into tropical biomes during the Paleocene, an epoch when both biomes are dominant in
254 North America. But North American tropical forests decline and then disappear
255 throughout the Oligocene and Miocene, extinguishing the opportunity for such a biome
256 shift during more recent times. The next section formalizes how we model the complex
257 interactions between biomes, regions, phylogeny, and time with these dynamics in mind.

258 *A time-stratified regional biome shift model*

259 The regional biome shift process may be viewed as a model that defines the
260 interactions (if any) of its two subprocesses, the biome shift process and the dispersal
261 process. We model biome shifts using a simple continuous-time Markov chain (CTMC)
262 with time-stratified rates (i.e. piecewise constant time-heterogeneous rate matrices; Ree
263 et al. 2005; Buerki et al. 2011; Bielejec et al. 2014; Landis 2017). Because transition rates
264 between regions depend in part on a lineage's biome affinity, and rates of shifting between
265 biomes depend in part on a lineage's geographical location, the two characters do not
266 evolve independently. To impose interdependence between biomes and regions, we define a
267 rate matrix over the compound state space using the approach of (Pagel 1994), while also
268 drawing on insights pioneered in newer trait-dependent models of discrete biogeography
269 (Sukumaran et al. 2015; Sukumaran and Knowles 2018; Matos-Maraví et al. 2018; Lu et al.
270 2019; Klaus and Matzke 2019).

271 Accordingly, we define the CTMC to operate on the compound biome-region state,
272 (i, k) , where i is the biome and k is the region. With this in mind, our goal is to compute
273 the probability of a lineage transitioning from biome i in region k to biome j in region l , or

274 (i, k) into (j, l). First, we take $\beta_{i,j}$ to model the shift rate between biomes i and j , and $\delta_{k,l}$
275 to model the dispersal rate between regions, $\delta_{k,l}$. Importantly, the values of β and δ
276 themselves do not directly depend on time. We eventually multiply these “base rates” by
277 time-dependent paleogeographical and paleoecological factors represented in our a
278 time-stratified (or epoch) model.

279 Computing the transition probabilities for an epoch model requires that we define
280 an instantaneous rate matrix $Q(m)$ for any supported epoch, m . Following Landis (2017),
281 we define the rate matrix $Q(m)$ as the weighted average of several rate matrices, each
282 capturing different paleogeographical features

$$Q(m) = w_1 Q_1 + w_G Q_G(m) + w_B Q_B(m). \quad (1)$$

283 The three matrices on the right-hand side of Equation 1 are the uniform rate
284 matrix, Q_1 , the geographical rate matrix, Q_G , and the biome rate matrix, Q_B . In reference
285 to Figure 2, we wish to learn the relative influence of the uniform (first column), geography
286 (second), and biome (third, fourth, or fifth) matrix features on the biome shift process.

287 The first rate matrix (Q_1) may be considered a “null” rate matrix that sets the
288 relative transition rates between all pairs of regions, and separately between all pairs of
289 biomes, as equal (to one).

$$[Q_1]_{(i,k),(j,l)} = \begin{cases} \beta_{i,j} & \text{if biome shift } (i \neq j) \\ \delta_{k,l} & \text{if region shift } (k \neq l) \\ 0 & \text{if biome and region shift } (i \neq j \text{ and } k \neq l) \end{cases}$$

290 The effect is that biome shifts between biomes i and j follow the rates $\beta_{i,j}$ and dispersal
291 events follow the rates $\delta_{k,l}$ regardless of the age of a lineage or the lineage’s biome-region
292 state. As we develop rate matrices for geography (Q_G) and and biomes (Q_B) below, the
293 second role for Q_1 is that it allows for lineages to disperse or shift regardless of whether the

294 connectivity/availability of the involved regions or biomes are scored as strong, weak, or
295 marginal.

296 The second rate matrix (indexed G for “geography”, Q_G) is structured according to
297 biome-independent paleogeographical features, such as the simple terrestrial connectivity
298 between regions. Connectivity is encoded as either as strong, weak or marginal in the
299 adjacency matrix, $A_G(m)$. Because we do not know precisely what, if any, influence strong,
300 weak, and marginal features should have upon the biome shift process, we allow each class
301 of features to have a range of (constrained) influences on the adjacency matrix.

302 Specifically, we set $y_{strong} = 1$ and $y_{marg} = 0$, then treat y_{weak} as an estimated parameter
303 that satisfies $y_{marg} < y_{weak} < y_{strong}$. Referring to Figure 2 again, these parameters control
304 the degree of contrast between cells across all matrices.

$$[Q_G(m)]_{(i,k),(j,l)} = \begin{cases} \beta_{i,j} & \text{if biome shift } (i \neq j) \\ \delta_{k,l} \times [A_G(m)]_{k,l} & \text{if region shift } (k \neq l) \\ 0 & \text{if biome and region shift } (i \neq j \text{ and } k \neq l) \end{cases}$$

305 The third rate matrix (indexed B for “biome”, Q_B) defines the shift rates between
306 biomes and the dispersal rates between regions to depend on the spatiotemporal
307 distribution of biomes. A lineage’s biome shift rate depends on whether the receiving
308 biome, j , has a strong, weak, or marginal presence in the region it currently occupies, k .
309 Likewise, the dispersal rate for a lineage that is currently adapted to biome type i depends
310 on whether the source region, k , and destination region, l , share a strong, weak, or

311 marginal connection.

$$[Q_B(m)]_{(i,k),(j,l)} = \begin{cases} \beta_{i,j} \times [A_j(m)]_{k,k} & \text{if biome shift } (i \neq j) \\ \delta_{k,l} \times [A_j(m)]_{k,l} & \text{if region shift } (k \neq l) \\ 0 & \text{if biome and region shift } (i \neq j \text{ and } k \neq l) \end{cases}$$

312 It is crucial to recognize that $Q_B(m)$ defines shift rates involving biome j to depend on the
 313 adjacency matrix for biome j during timeslice m . This key property means that lineages
 314 currently adapted to biome j disperse with rates according to the interregional connectivity
 315 of biome j , and lineages newly adapting to biome j do so at a rate depending on the local
 316 availability of biome j .

317 The transition rates (and probabilities) between biome-region pairs are not expected
 318 to be symmetrically equal across time intervals. For example, if biome j first appears in
 319 region k during time interval $m + 1$ then we see an increase in the biome shift rate, i.e.
 320 $[Q(m)]_{(i,k),(j,k)} < [Q(m+1)]_{(i,k),(j,k)}$. Nor are transition rates necessarily symmetrically
 321 equal within a given time interval. If region k contains biome i during time interval m , but
 322 region l does not, then we find that lineages adapted to biome i disperse more easily from k
 323 into l than l into k , i.e. $[Q(m)]_{(i,k),(i,l)} < [Q(m)]_{(i,l),(i,k)}$. Similarly, if region k contains
 324 biome i but not biome j , then lineages inhabiting region k tend to shift more easily from
 325 biome i into j than from j into i , i.e. $[Q(m)]_{(i,k),(j,k)} < [Q(m)]_{(j,k),(i,k)}$.

326 Fluctuating asymmetries in the rates over time means that each biome-region state
 327 may exhibit different source-sink dynamics across that timescale. During a period of low
 328 accessibility, a biome-region state might rebuff immigrants and lose occupants (and so act
 329 as a source) but then gain and retain inhabitants during a later phase should that
 330 biome-region become a local refugium (and so act as a sink) (Goldberg et al. 2005). These
 331 fluctuating source-sink dynamics may be characterized by the stationary distribution,
 332 which defines the expected proportion of lineages found in each biome-region state

³³³ assuming lineages evolve along an infinitely long branch within a given time interval.
³³⁴ Biome-regions that are easy to enter and difficult to leave tend towards higher stationary
³³⁵ probabilities for a given time interval. We approximate the stationary probability for
³³⁶ biome i in region k during epoch m with

$$\pi(m)_{(i,k)} = [e^{\mu Q(m)}]_{1,(i,k)}$$

³³⁷ where μ is a rate taken to be sufficiently large that stationarity is reached. We validate
³³⁸ that all rows have arbitrarily similar transition probabilities, which lets us take any row
³³⁹ (i.e. the first row) to represent the stationary probabilities.

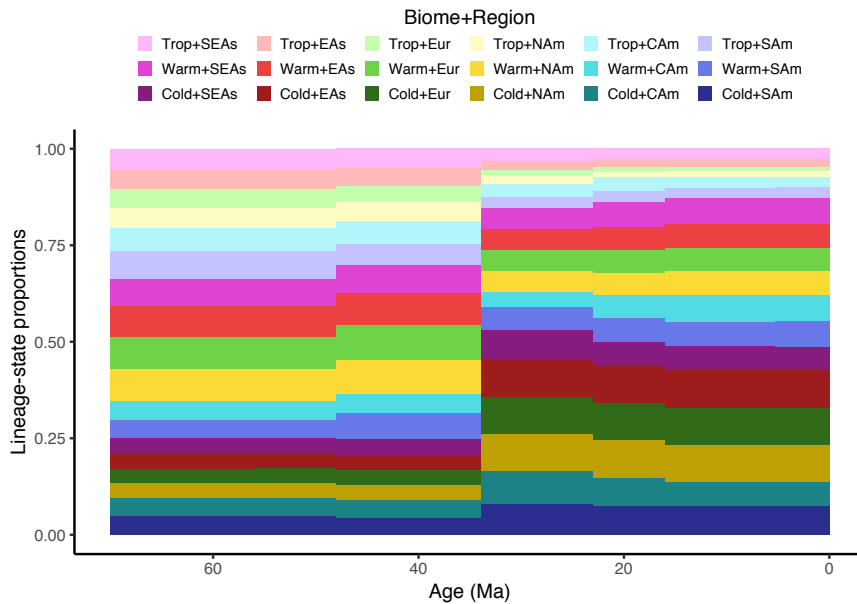


Figure 3: Stationary distribution of biome-region states under the paleobiome model. The stationary probabilities across biome-regions (y-axis) vary with respect to time (x-axis). Stationary probabilities were computed assuming that biome and region shifts occur in roughly equal proportion ($\beta = \delta = 0.5$), that lineages disperse primarily through the appropriate biome graph ($w_B = 0.8$, $w_G = 0.16$, and $w_1 = 0.04$), and that dominant biomes primarily define the structure of biome graphs ($y_{strong} = 1.0$, $y_{weak} = 0.1$, $y_{marg} = 0.0$). Parameters were chosen to show interesting variation. Note, all stationary probabilities would be equal over all times if $w_1 = 1$.

³⁴⁰ The time-dependent source-sink dynamics in Figure 3 show how the availability of
³⁴¹ and connectivity between regional biomes structures each time interval's stationary

³⁴² distribution. Stationary probabilities before the Oligocene tend to favor tropical biomes in
³⁴³ all regions, but favor cold temperate biomes afterwards. This means that if the historical
³⁴⁴ spatial structure of biomes is relevant to biogeography, then lineages originating in the
³⁴⁵ Paleogene would more likely be adapted to tropical than to cold temperate forests simply
³⁴⁶ because cold temperate forests were a more marginal biome during that period of Earth's
³⁴⁷ history.

³⁴⁸ We can now completely define the time stratified rate matrix, $Q(m)$, and the
³⁴⁹ stationary frequencies at the root of a phylogeny, $\pi(m_{root})$, where m_{root} is the epoch index
³⁵⁰ corresponding to the root node age. Together, these model components let us compute the
³⁵¹ probabilities of lineages transitioning from one biome-region pair to another while
³⁵² accounting for the spatiotemporal dynamics of biomes, and thus compute the phylogenetic
³⁵³ model likelihood with the discrete state pruning algorithm (Felsenstein 1981).

³⁵⁴ Now that we have fully defined the model, there are several implicit properties that
³⁵⁵ are worth stating explicitly. First, a lineage cannot both shift its biome affinity and
³⁵⁶ disperse into a new region in the same moment of time; one event is needed for each
³⁵⁷ transition, and so event order matters. Second, the relative importance of the matrix
³⁵⁸ feature weights (w_1, w_G, w_B) and of the availability/connectivity weights (y_{weak}) are
³⁵⁹ estimated from the data: the matrix $Q(m)$ reduces to the “null” matrix $Q_1(m)$ when
³⁶⁰ $w_1 = 1$, while the importance of the historical structure of biomes is most pronounced
³⁶¹ when w_B and y_{strong} are large compared to other w and y parameters. Third, the process
³⁶² models lineages as being predominantly present in a single region and biome at a time
³⁶³ without influencing speciation or global extinction rates, both to simplify the exposition of
³⁶⁴ the method, but also to reduce computational burden. The Discussion pays more attention
³⁶⁵ to these properties.

³⁶⁶ *Bayesian inference*

³⁶⁷ The Bayesian posterior density was estimated using the Markov chain Monte Carlo

368 (MCMC) algorithm implemented in RevBayes (Höhna et al. 2016). The first 50% of
369 posterior samples were discarded as burn-in. All parameter estimates have effective sample
370 sizes well over 200. Two independent chains were run per analysis to verify MCMC
371 convergence. We analyzed our data under three model settings: the *Paleobiome* setting
372 that used the time-heterogeneous graphical structure presented in Figure 2; the *Modern*
373 *Biome* setting that used the graphical structure of “Present” to represent all time intervals;
374 and the *Null Biome* setting that ignored all regional and biome structure by fixing $w_1 = 1$.

375 Departing from the general model description above, we re-parameterized our
376 applied model to eliminate informative priors wherever possible. This helped ensure that
377 our posterior estimates are driven by the data through the likelihood function, not the
378 prior. We assigned uninformative prior distributions to our graph weights,
379 $(w_1, w_L, w_B) \sim \text{Dirichlet}(1, 1, 1)$, and to our graph feature strength parameter,
380 $y_{weak} \sim \text{Uniform}(0, 1)$. We treated each biome shift rate as an independently estimated
381 parameter, $\beta_{i,j} \sim \text{Uniform}(0, 1)$, but fixed the biome shift rate between tropical and cold
382 temperate biomes equal to zero. Because we already constrained biome-independent
383 dispersal between regions through graphical structures (Q_G) and weight parameters (w_1
384 and w_G), we fixed the relative dispersal rate to $\delta_{k,l} = 1$ (which is potentially rescaled by Q_G
385 and w_G). Thus, the relative biome shift rates β and dispersal rates δ have values between 0
386 and 1. To balance the relative proportion of biome shifts to dispersal events, we multiply β
387 by the factor $f_\beta \sim \text{Uniform}(0, 1)$ and multiply δ by $f_\delta = (1 - f_\beta)$. Finally, we rescaled the
388 instantaneous rate matrix, Q , for the entire evolutionary process by a global clock
389 parameter, $\mu \sim \text{LogUniform}(10^{-4}, 10^1)$, that is uniformly distributed over orders of
390 magnitude.

391 We summarized our results in several ways. Ancestral state estimates show the
392 posterior probability for each node’s biome-region state. Only the three most probable
393 states are shown, with all less probable states and their probabilities collapsed into a single
394 ‘?’ state. The ancestral biome-region state for the root node is magnified to improve

395 visibility.

396 Lineage-state through time estimates are computed from posterior distributions of
397 stochastically mapped histories. We computed the posterior mean count of lineage-states
398 through time as the number of lineages in each state for each time bin across posterior
399 samples divided by the total number of posterior samples. Lineage-state counts were
400 converted into lineage-state proportions by dividing each count by the total number of
401 lineages in that time bin to give proportions that lie between 0 and 1. In addition, we
402 classified whether or not each lineage-state for each time bin was congruent with any
403 locally prominent biome as defined by the paleobiome graph (Fig 2). Each binned state
404 was labeled as a *biome mismatch* if the lineage's biome was only marginally present in the
405 lineage's region. Otherwise, the state was labelled as a *biome match*. To summarize these
406 results, we also computed the proportion of tree length where lineage states match or
407 mismatch paleobiome structure in three ways: for the total tree length, for tree length
408 before the Oligocene (>34 Ma) and for tree length after the Oligocene (≤ 34 Ma).

409 Finally, we were interested in the ordered *event series* that resulted in major
410 transitions between biomes and regions. For biomes A , B , and C and regions X , Y , and Z ,
411 we named the six series patterns for pairs of events. Series in which species shift biomes
412 and then disperse ($AX \rightarrow BX \rightarrow BY$) are called *biome-first* event series. In contrast,
413 *region-first* series have dispersal followed by a biome shift event ($AX \rightarrow AY \rightarrow BY$). The
414 remaining four event series involve two consecutive biome shift or two dispersal events.
415 *Biome reversal* ($AX \rightarrow BX \rightarrow AX$) and *region reversal* ($AX \rightarrow AY \rightarrow AX$) sequences
416 indicate event series in which the lineage departs from and then returns to its initial state
417 (AX). Analogously, *biome flight* ($AX \rightarrow BX \rightarrow CX$) and *region flight* ($AX \rightarrow AY \rightarrow AZ$)
418 sequences are recognized by series of two biome shifts or two dispersal events that leave the
419 lineage in a new state (CX or AZ) relative to the lineage's initial state (AX). We
420 computed the proportion of each series type for a single posterior sample by classifying
421 stochastically mapped state triplets (event series of length two) in our phylogenetic tree

422 using a simple root-to-tip recursion. We processed each posterior sample by taking the
423 stochastically mapped root state to be the second state in the triplet, X_{root} , then sampling
424 the preceding state, $X_{subroot}$, from the sampling distribution obtained by Bayes rule

$$P(X_{subroot} = (i, k) | X_{root} = (j, l), Q(m_{root})) \propto \frac{[Q(m_{root})]_{(i,k),(j,l)}}{\sum_{(x,y) \neq (i,k)} [Q(m_{root})]_{(i,k),(x,y)}} \times \frac{[\pi(m_{root})]_{(i,k)}}{[\pi(m_{root})]_{(j,l)}}$$

425 where $Q(m_{root})$ is the root node's rate matrix and $\pi(m_{root})$ is its stationary distribution
426 with values determined by the evaluated posterior sample. Following that, we executed a
427 recursion towards the tips of the tree to collect changes in the stochastic mapping for each
428 lineage's biome-region state, classifying the state triplet's type, and updating the triplet
429 states appropriately (i.e. the new second and third states replace the old first and second
430 states) with each step of the recursion.

431 Finally, we wished to examine if and how the distribution of evolutionary events
432 changed with time under alternative assumptions about the biome structure. We were
433 particularly interested in two classes of event proportions: proportions of various types of
434 biome shift and dispersal events, and proportions of the various types of event series. To
435 estimate the proportions of biome shift and dispersal event types through time, we
436 computed the posterior mean count for each distinct biome shift and dispersal event type
437 per 1 Myr interval, then divided that count of each interval by the total number of events
438 per interval. Although we normalized our proportions using all 126 distinct dispersal and
439 biome shift event types, our results only display the four biome shift and four dispersal
440 event types among all combinations of the warm and cold temperate forests of East Asia
441 and North America. In a similar manner, we computed the posterior proportions for all six
442 types of event series, using the time of the second event in each series for each series age.
443 Our presented event and event series proportions through time were smoothed by a locally
444 estimated smoothing regression (LOESS) using `ggplot2` (Wickham 2016). After
445 smoothing, confidence intervals were truncated at zero to exclude rare events from having

446 negative proportions.

447 *Simulation experiment*

448 We measured how reliably we can select models in which biome structure influences the
449 biome shift process ($w_B > 0$) for *Viburnum* with simulated data. All simulations assumed
450 the same *Viburnum* phylogeny used in the empirical example and used the same biome and
451 regions designated by the paleobiome structure model. We simulated data under five
452 conditions that primarily adjust the relative weight for w_B , named: null effect, where
453 $(w_1, w_G, w_B) = (1, 0, 0)$; weak effect, where $(w_1, w_G, w_B) = (1, 2, 4)/7$; medium effect, where
454 $(w_1, w_G, w_B) = (1, 2, 8)/11$; strong effect, where $(w_1, w_G, w_B) = (1, 2, 16)/19$; and very
455 strong effect, where $(w_1, w_G, w_B) = (1, 2, 32)/35$; with each denominator ensuring the
456 weights sum to 1. For all conditions, we assumed $f_\beta = 0.75$, $f_\delta = 0.25$, and $y_{weak} = 0.1$.
457 Biome shift rates were set to equal 1, except transitions between cold temperate and
458 tropical forests, which were set to 0. The event clock was set to $\mu = 0.03$, except for the
459 null condition, which was assigned a slower rate of $\mu = 0.01$ to account for the fact that
460 fewer event rate penalties are applied to it than the non-null conditions. We then
461 simulated 100 replicate datasets in RevBayes for each of the four conditions under the
462 regional biome-shift model described above, and estimated the posterior density for each
463 simulated dataset using MCMC in RevBayes.

464 We were primarily concerned with how our posterior estimates of w_B respond to
465 differing simulated values for w_B . To summarize this, we first report the posterior median
466 values of w_B across replicates so they may be compared to the true simulating value. Next,
467 we computed what proportion of our replicates select a complex model allowing $w_B > 0$ in
468 favor of a simpler model where $w_B = 0$ using Bayes factors. Bayes factors were computed
469 using the Savage-Dickey ratio (Verdinelli and Wasserman 1995), defined as the ratio of the
470 prior probability divided by the posterior probability, evaluated at the point where the
471 complex model collapses into the simpler model (i.e. $w_B = 0$, in our case). We interpret

472 the strength of significance for Bayes factors as proposed by Jeffreys (1961), requiring at
473 least ‘Substantial’ support ($BF > 3$) to select the more complex model ($w_B > 0$).

474

RESULTS

475

Simulation experiment

476 Simulated datasets yielded larger estimates of w_B and more soundly rejected null
477 models ($w_B = 0$) as the effect strength w_B increased from Weak to Very Strong (Fig. 4).
478 No datasets simulated under the Null condition ($w_B = 0$) signalled Substantial support (or
479 greater) for the paleobiome-dependent model ($w_B > 0$), indicating a low false positive rate.
480 Only 9% of datasets simulated under Weak effects ($w_B = 4/7 \approx 0.57$) generated No
481 support for the $w_B > 0$ model, and only $\sim 32\%$ of those replicates qualified as Substantial
482 support or greater. Data simulated under the Moderate condition ($w_B = 8/11 \approx 0.73$)
483 reject the simple model 57% of the time with at least Substantial support. Under Strong
484 ($w_B = 16/19 \approx 0.84$) simulation conditions, we selected models where $w_B > 0$ in 81% of
485 cases, with Strong support in 65% of cases. Data simulated under Very Strong effects
486 ($w_B = 32/35 \approx 0.91$) generated support for models with $w_B > 0$ 88% of the time, with over
487 half of all replicates (54%) drawing Very Strong or Decisive support. Coverage frequency
488 among simulations was consistently high across conditions, but with fairly wide HPD95
489 credible intervals (Fig. 4A). Because the posterior probability of $w_B = 0$ is used to
490 approximate Bayes factor ratios, their relationship is made apparent by noting that the
491 density of HPD95 lower bound estimates close to the value $w_B = 0$ (Fig. 4A) is correlated
492 with the proportion of simulations that award no support to the $w_B > 0$ model (Fig 4B).

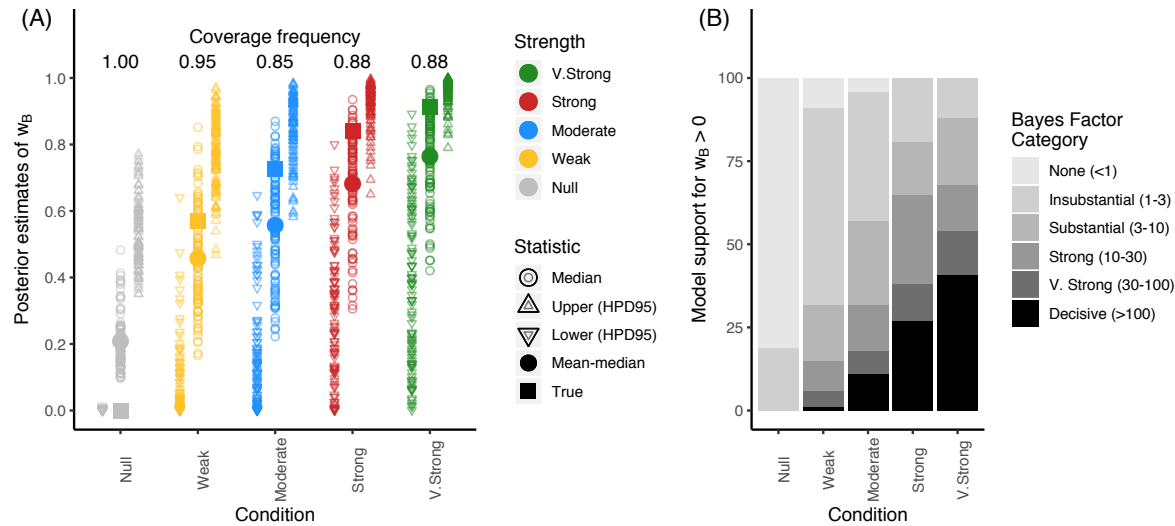


Figure 4: Simulation experiment results. One hundred datasets were simulated under five conditions that varied the strength of w_B , then fitted to the paleobiome model to assess model performance. (A) Markers show the true simulated strength for w_B (closed square), the posterior median values estimated from simulated replicates (open circles), the median of those posterior medians (closed circle), and the upper and lower bounds of the 95% highest posterior density (open triangles). The coverage frequency reports the proportion of simulation analyses in which the simulating value of w_B is falls within the credible interval. (B) Bars report the proportions of simulated datasets that supported the model where $w_B > 0$, categorized by the strength of that support in terms of Bayes factors (Jeffreys 1961).

494 Although *Viburnum* likely originated in East Asia regardless of the biome structure model
 495 ($p > 0.99$), no model reconstructed a single ancestral biome affinity with probability
 496 greater than $p > 0.95$ (Figure 5). Where the *Paleobiome* analysis inferred East Asian
 497 biome affinities that favored a warm temperate ($p = 0.88$) or tropical ($p = 0.09$) but not a
 498 cold temperate ($p = 0.03$) origin, the *Modern Biome* analysis favored a cold temperate
 499 ($p = 0.67$) then warm temperate ($p = 0.31$) origin for *Viburnum* while assigning negligible
 500 probability to a tropical origin ($p = 0.01$). Relative to the *Paleobiome* estimates, the *Null*
 501 *Biome* analysis also assigned higher probabilities to colder biomes (warm, $p = 0.52$; warm,
 502 $p = 0.45$; tropical, $p = 0.02$). Early diverging *Viburnum* lineages tended to follow
 503 warm/tropical biome affinities under the *Paleobiome* analysis or the cold/warm affinities
 504 under the *Modern/Null Biome* analyses before the Oligocene (>34 Ma). During the
 505 Oligocene (34–22 Ma), when cold temperate forests first expanded, many nodes still

506 retained the warmer or colder biome affinities characteristic of the biome structure model,
507 such as the most recent common ancestor (MRCA) of *V. reticulatum* and *V. ellipticum* or
508 the MRCA of *V. rufidulum* and *V. cassinooides*. Otherwise, most ancestral biome inferences
509 were consistent across the three models, beginning with the Mid/Late Miocene (<16 Ma).

510 Figure 6A–C shows that the three biome structures recovered different proportions
511 of ancestral lineage-states through time, particularly before the Mid/Late Miocene (>16
512 Ma). Between the Paleocene and the Early Miocene, tropical lineages in East Asia and
513 Southeast Asia constituted >20% diversity, declining to ~12% of modern diversity under
514 the *Paleobiome* analysis. Cold temperate lineages were nearly absent until the end of the
515 Oligocene (34 Ma), but steadily rose to constitute roughly 25% of diversity by the
516 Early/Mid Miocene (ca. 20 Ma). By comparison, *Modern Biome* estimates enriched the
517 proportion of cold temperate viburnums, while reducing support for warm temperate and
518 nearly eliminating support for tropical origins; tropical lineages remained in comparatively
519 low proportion until the Miocene (< 22 Ma). The *Null Biome* analysis estimated
520 proportions of warm and cold temperate lineages similar to those of the *Modern Biome*
521 analysis from the Late Cretaceous (100 Ma) until the Oligocene (34 Ma), but with more
522 Southeast Asian warm temperate lineages throughout.

523 For what proportion of time did lineages have biome affinities that were congruent
524 with locally accessible biomes? Biomes rarely mismatched between lineages and regions
525 under the *Paleobiome* setting (1.1% of tree length), with the mismatches increasing under
526 the *Modern Biome* (8.6%) and *Null Biome* (8.7%) settings. Lineages were most often
527 mismatched with their regions' biomes before the Oligocene (Figures 6D–F), where the
528 pre-Oligocene proportion of mismatched branch lengths was always higher (*Paleobiome*,
529 5.8%; *Modern Biome*, 52.6%; *Null Biome*, 47.1%) than the post-Oligocene proportion
530 (*Paleobiome*, 0.3%; *Modern Biome*, 0.8%; *Null Biome*, 1.7%) or the treewide proportions
531 (above).

532 To illuminate why the *Paleobiome* analysis produces distinctly warmer ancestral

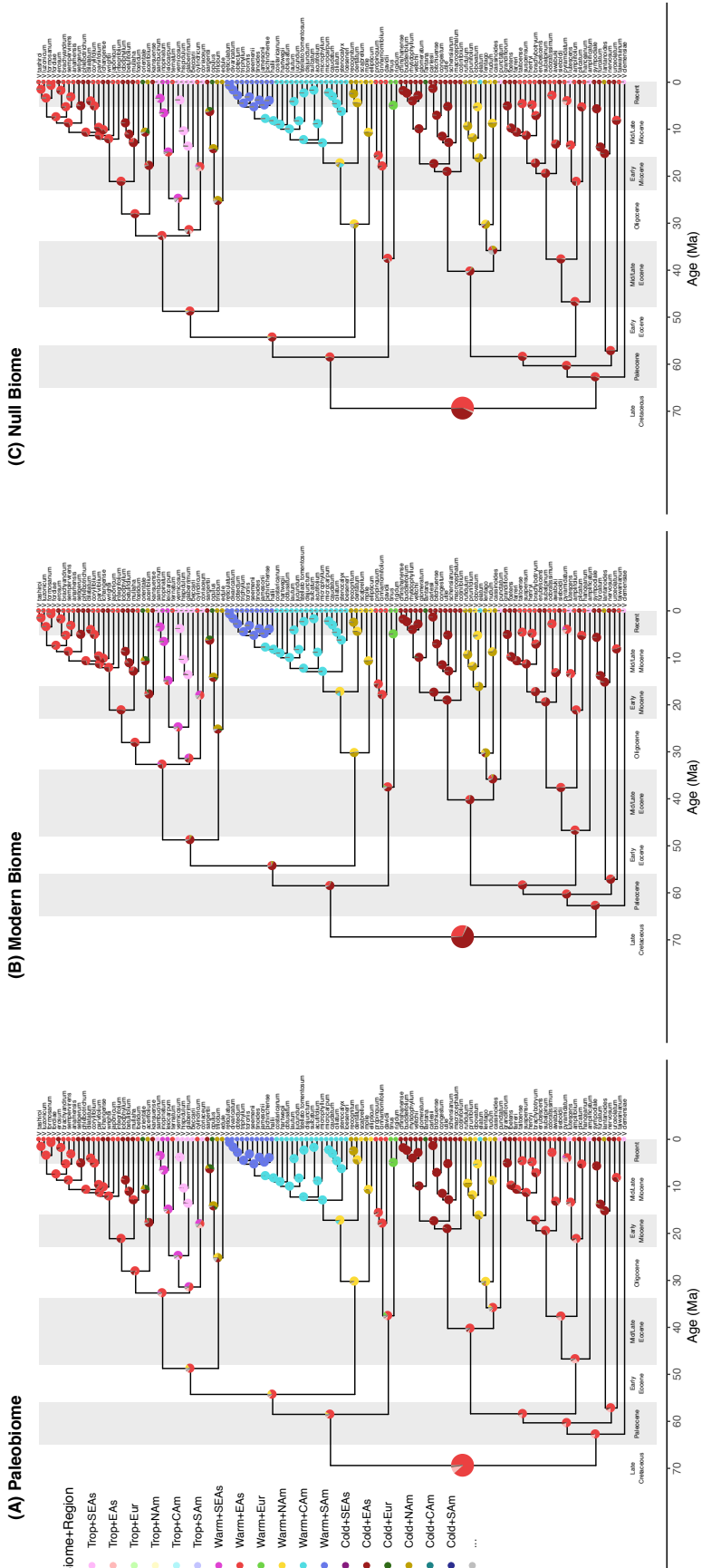


Figure 5: Ancestral biome-region state estimates for *Viburnum* under the time-stratified regional biome shift model. Estimates produced under (A) *Paleobiome*, (B) *Modern Biome*, and (C) *Null Biome* settings. Colored pie charts report posterior support for the most probable biome-region states per node. Pie charts for root state probabilities are magnified to improve visibility. Vertical white and gray bands correspond to major geological timeframes referenced in this study.

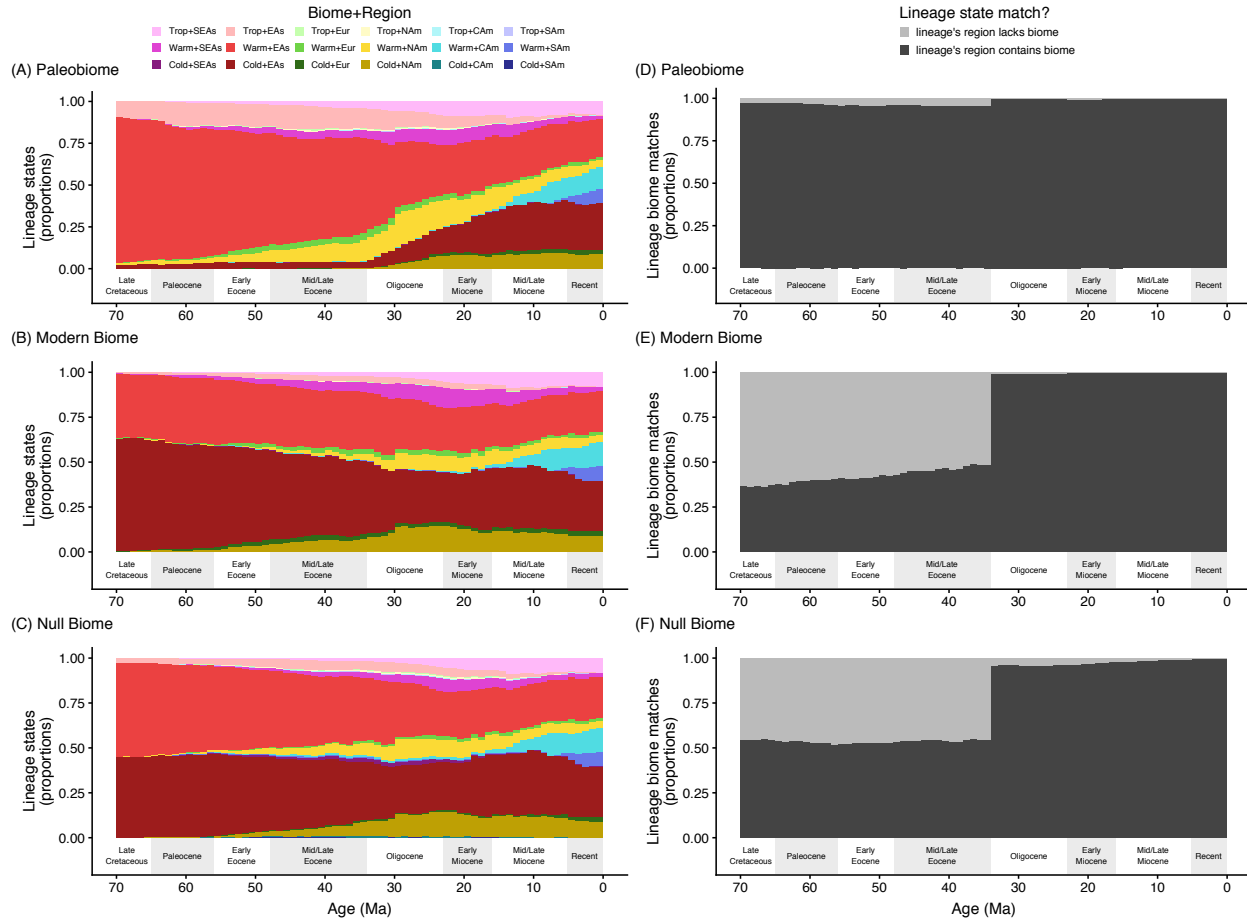


Figure 6: Proportions of ancestral *Viburnum* lineages with biome-region state frequencies through time. The left column (A–C) shows the lineages biome-region states, where regions differ by color and biomes differ by shading (see legend). Proportions of reconstructed lineages in each biome-region state are shown for estimates under the *Paleobiome* (A), *Modern Biome* (B), and *Null Biome* (C) settings. The right column (D–F) shows the proportion of lineages with biome states that “match” (dark) or “mismatch” (light) the non-marginal biomes that are locally accessible given any lineage’s location, as defined under the *Paleobiome* structure (see main text for details). Proportions of reconstructed lineages with biome match and mismatch scores are shown for estimates under the *Paleobiome* (D), *Modern Biome* (E), and *Null Biome* (F) settings.

533 biome estimates, we turn to the fitted stationary probability for the root state, $\pi(m_{\text{root}})$,
 534 (Figure 7). Within East Asia, root node stationary probabilities estimated under the
 535 *Paleobiome* setting favored warm temperate or tropical forests over cold temperate forests
 536 ($\pi_{\text{Trop+EAs}} = 0.06, \pi_{\text{Warm+EAs}} = 0.10, \pi_{\text{Cold+EAs}} = 0.02$). The *Modern Biome* stationary
 537 probabilities instead favored cold or warm temperate forests over tropical forests

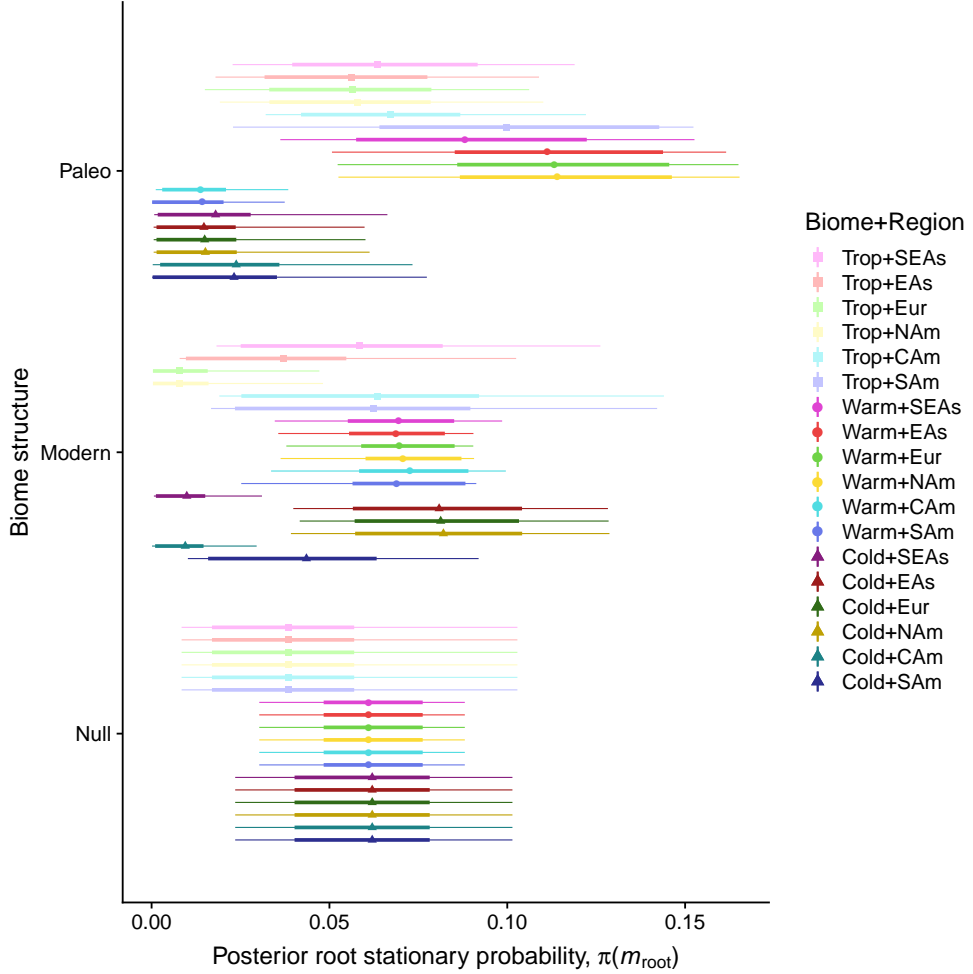


Figure 7: Stationary probabilities at root node during the Late Cretaceous. Posterior stationary probabilities for $\pi(m_{\text{root}})$ are given for each biome structure model biome-region state (rows) and for each biome+region state (colors) as posterior medians (points) and credible intervals (HPD70, thick lines; HPD95, thin lines).

538 ($\pi_{\text{Trop+EAs}} = 0.03, \pi_{\text{Warm+EAs}} = 0.07, \pi_{\text{Cold+EAs}} = 0.08$). Like the *Modern Biome* analysis,
 539 stationary probabilities under the *Null Biome* setting tended towards cold or warm
 540 temperatures ($\pi_{\text{Trop+EAs}} = 0.04, \pi_{\text{Warm+EAs}} = 0.06, \pi_{\text{Cold+EAs}} = 0.06$), noting that the
 541 stationary probability per biome is uniform across regions by the design of the model.

542 Despite such differences between the *Paleobiome* and *Modern Biome* analyses in
 543 their ancestral state estimates and stationary probabilities, their parameter estimates for
 544 the base rate of change (μ), the proportion of biome shifts (f_β) to dispersal events (f_δ), and
 545 the graph weights (w_1, w_G, w_B) were remarkably similar (Table 1). Both biome structure

Parameter	Biome structure		
	Paleo	Modern	Null
μ	0.06 [0.03, 0.10]	0.05 [0.03, 0.09]	0.03 [0.02, 0.06]
f_β	0.85 [0.75, 0.94]	0.83 [0.69, 0.93]	0.92 [0.85, 0.97]
f_δ	0.15 [0.06, 0.25]	0.17 [0.07, 0.31]	0.08 [0.03, 0.15]
β_{TW}	0.67 [0.20, 1.00]	0.50 [0.05, 0.95]	0.54 [0.10, 1.00]
β_{WC}	0.81 [0.47, 1.00]	0.81 [0.48, 1.00]	0.74 [0.39, 1.00]
β_{CW}	0.28 [0.09, 0.62]	0.39 [0.11, 0.85]	0.31 [0.08, 0.66]
β_{WT}	0.38 [0.01, 0.80]	0.65 [0.34, 1.00]	0.72 [0.33, 1.00]
w_1	0.01 [0.00, 0.07]	0.02 [0.00, 0.08]	1
w_G	0.04 [0.00, 0.18]	0.04 [0.00, 0.20]	0
w_B	0.94 [0.78, 1.00]	0.93 [0.76, 1.00]	0
y_{weak}	0.65 [0.27, 0.99]	0.52 [0.09, 0.95]	1

Table 1: Regional biome shift parameter estimates. Posterior median estimates are in bold and 95% highest posterior densities are in brackets. Fixed parameters under the *Null Biome* analysis do not have brackets.

models estimate posterior means for w_B greater than 0.91; i.e., stronger in effect than assumed under the Very Strong simulation scenario (Figure 4). Both models estimated credible intervals for w_B with lower bounds greater than 0.75 and posterior probabilities of $w_B = 0$ that were indistinguishable from zero, each corresponding to “Decisive” support for their respective biome structure models. Because inference under the *Null Biome* model set $y_{weak} = 1$, posterior estimates of (w_1, w_G, w_B) are indistinguishable from the prior. Parameter estimates for the relative biome shift rates differed across the three biome structure models, however. The *Paleobiome* estimates favor hot-to-cold shifts ($\beta_{TW} = 0.63 > \beta_{WT} = 0.43$ and $\beta_{WC} = 0.82 > \beta_{CW} = 0.29$) while the *Modern Biome*

estimates favor shifts leaving the warm temperate biome ($\beta_{TW} = 0.44 < \beta_{WT} = 0.65$ and $\beta_{WC} = 0.80 > \beta_{CW} = 0.42$), as do the *Null Biome* estimates ($\beta_{TW} = 0.55 < \beta_{WT} = 0.76$ and $\beta_{WC} = 0.73 > \beta_{CW} = 0.32$).

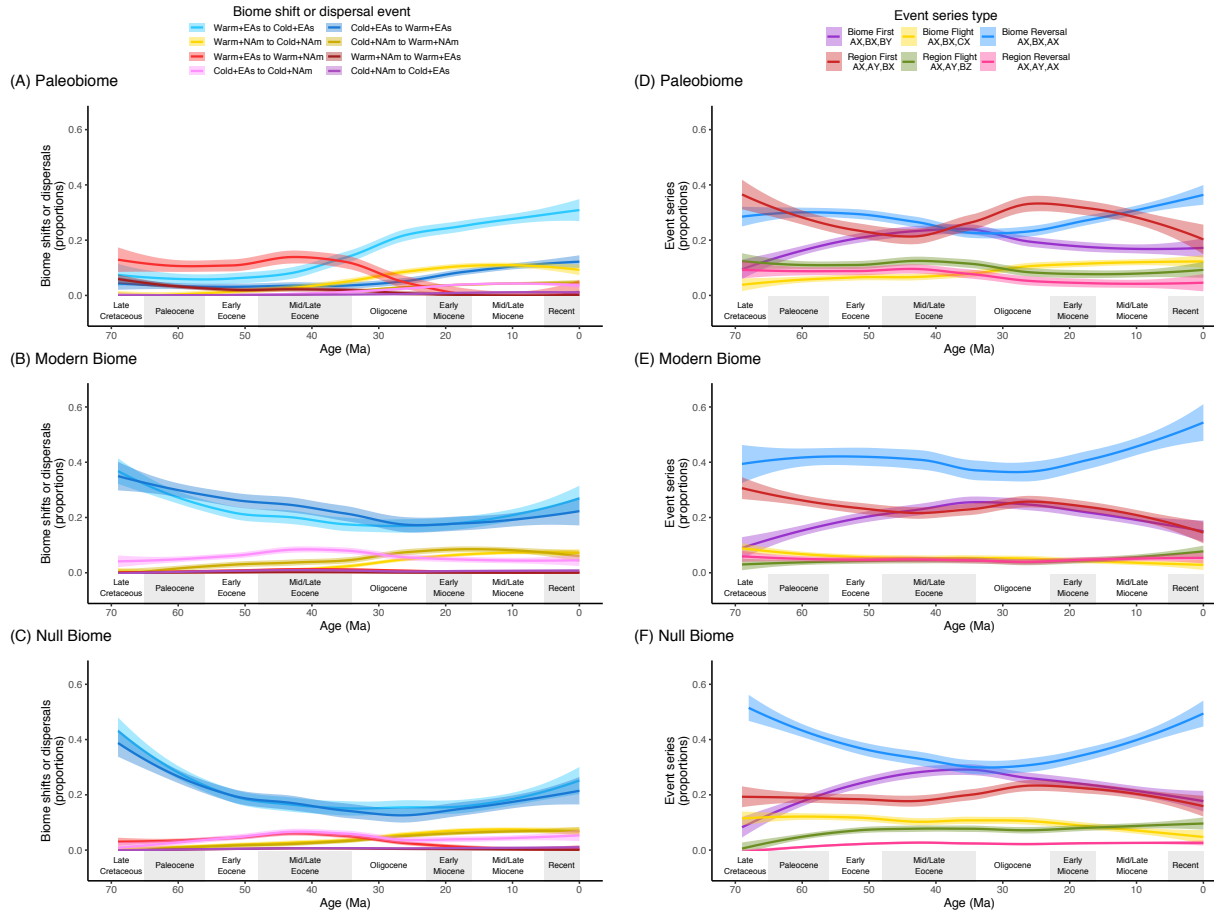


Figure 8: Smoothed proportions of inferred events and event series through time for *Viburnum*. The left column (A–C) presents the proportions of estimated biome shift and dispersal events with respect to time, showing only the eight biome shift and dispersal events among the warm and cold temperate forests of East Asia and North America. Proportions of events are shown for inferences under the *Paleobiome* (A), *Modern Biome* (B), and *Null Biome* (C) settings. The right column (D–F) shows the proportions of the six types of event series with respect to time (defined in main text). Each event series type is labeled with a ‘state triplet’ to indicate either transitions in the biome (A, B, C) or region (X, Y, Z) state. Proportions of event series are shown for inferences under the *Paleobiome* (D), *Modern Biome* (E), and *Null Biome* (F) settings.

Finally, we found that the *Paleobiome* analysis estimated proportions of biome shift and dispersal events that are more temporally dynamic than those proportions estimated

560 under the *Modern Biome* and *Null Biome* models (Fig. 8A–C). Under the *Paleobiome*
561 estimates, dispersal events from East Asia into North America within the warm temperate
562 biome were relatively common throughout the Late Eocene. With the onset of Oligocene
563 cooling, biome shifts from warm into cold temperate forests in East Asia rose from low to
564 high proportions to become the most frequent transition type. In contrast, event
565 proportions under the *Modern Biome* and *Null Biome* analyses reconstructed high
566 proportions of biome shifts between the warm and cold temperate forests of East Asia since
567 *Viburnum* first originated in the Late Cretaceous through the present. Paleocene dispersal
568 of cold temperate lineages from East Asia into North America was also found to be
569 relatively common when compared to the *Paleobiome* reconstruction. Regarding the event
570 series proportions, biome reversal, biome-first, and region-first series were generally more
571 common than biome flight, region flight, and region reversal series (Fig. 8). The biome
572 reversal event series was the most common event series type across all time intervals under
573 the *Modern Biome* and *Null Biome* analyses, but not under the *Paleobiome* analysis. With
574 the *Paleobiome* model, we found that the proportion of biome reversal series was lower,
575 and the proportion of region-first series was higher, when compared to the other biome
576 structure analyses, together creating a time interval between the Late Eocene and the
577 Middle Miocene during which region-first events outpaced all other types of series.

578 DISCUSSION

579 The probability that a lineage will shift into a new biome is determined in part by
580 geographical opportunities. Because the availability and connectivity of biomes varies
581 across regions, evolutionary lineages do not share the same geographical opportunities to
582 adapt to new biomes. Moreover, those geographical opportunities have changed as the
583 spatial structure of Earth's biomes evolved over time. As an evolutionary inference
584 problem, the temporal dynamics of geographical opportunity is concerning: we typically
585 infer ancestral biomes based on the phylogenetic distribution of biomes from extant species,

586 yet their ancestors were likely exposed to geographical opportunities significantly (perhaps
587 even radically) different from the opportunities of their living descendants.

588 Here, we have developed a Bayesian framework to model how phylogenetic lineages
589 gain affinities with new biomes and disperse between regions in a manner reflecting the
590 historical configuration of biomes through space and time. To do so, we modeled a
591 time-stratified biome-region shift process using continuous-time Markov chains. The model
592 is parameterized to allow biome shift and dispersal rates to depend on empirically
593 structured paleobiome graphs, where each graph describes the availability and connectivity
594 of biomes among regions within a given time stratum. We conducted a simple simulation
595 experiment to show that we can identify which comparative datasets were shaped by
596 paleobiome structure ($w_B > 0$) using Bayes factors, provided the strength of the effect was
597 at least moderately strong, even though w_B is difficult to estimate precisely (Fig. 4). We
598 then fitted our new model to estimate ancestral biomes and regions for *Viburnum*. In
599 discussing our results, we focus on two principal aspects of our study: first, our empirical
600 findings in *Viburnum* and how these may inform other studies seeking to estimate ancestral
601 biomes or regions; and, second, an examination of the model's assumptions and properties,
602 and how the model's realism may be improved in future work.

603 *Biome shifts in Viburnum*

604 *Viburnum* first diversified the Paleocene and Eocene (66–34 Ma), a period when
605 boreotropical forests dominated and connected the northern continents (Wolfe 1985;
606 Graham 2011; Willis and McElwain 2014). Cold temperate forests that experienced long
607 freezing periods were globally rare until after the Oligocene (<34 Ma). Although we
608 inferred an East Asian origin regardless of what biome structure model was assumed,
609 ancestral biome estimates under the three structure models differed in important ways. In
610 the *Paleobiome* analysis, the ancestral biome of the crown node was probably warm
611 temperate ($p = 0.88$) and possibly tropical ($p = 0.09$), and a cold temperate origin could

decisively be ruled out ($p < 0.05$; Fig. 5A). When we assumed that biome structure had always resembled today's structure (*Modern Biome*), the crown node support changed, instead favoring a cold temperate ($p = 0.67$) or possibly a warm temperate ($p = 0.31$) origin (Fig. 5B). The *Null Biome* reconstruction also recovered a warm ($p = 0.52$) or cold ($p = 0.45$) temperate origin, despite the fact that the *Null Biome* inference assumed that all biomes are present in all regions at all times. Mismatches between lineage biome affinities and regionally available biomes were highest among pre-Oligocene lineages (>34 Ma). Though cold temperate lineages remained in low proportions (~5%) until the Oligocene under the *Paleobiome* analysis (Fig. 6A), the *Modern/Null Biome* analyses maintained high proportions of cold temperate lineages in East Asia (> 30%) and North America (7%) in the Eocene (Fig. 6B,C). Over 53% and 47% of pre-Oligocene branches bore mismatched biomes under the *Modern* and *Null Biome* analyses, respectively, but only 6% of those branch lengths were mismatched with biomes under the *Paleobiome* model (Figures 6D–F). Because of the global rarity of the cold temperate biome during the period of early *Viburnum* evolution, we favored the warm temperate or tropical origin of *Viburnum* under the *Paleobiome* analysis.

Yet, despite stark differences in the *Paleobiome* and *Modern Biome* models, parameter estimates under both conditions found the spatial distribution of biomes to be the primary factor in explaining how viburnums came to live where they do today ($w_B > 0.92$, i.e. compatible with the Very Strong condition used in the simulation experiment). Because the ability to estimate ancestral states or to fit evolutionary parameters decays as the evolutionary timescale deepens, we expect that both the *Paleobiome* and *Modern Biome* analyses primarily fit their parameters to phylogenetic patterns of variation pronounced at the shallowest timescales. All else being equal, however, older *Viburnum* lineages should disperse and biome shift in a manner that is similarly limited by geographical opportunities. The static geographical opportunities assumed under the *Modern Biome* structure induced stationary probabilities that project

639 today's colder conditions back into the Late Cretaceous, while the dynamic *Paleobiome*
640 structure favored hotter conditions unlike those at present (Figures 2 and 7). The lesson
641 we take from this is that inferring the fundamental behavior of the process is not always
642 sufficient for estimating ancestral states; inferring if and how that behavior responds to
643 changing historical conditions is also necessary.

644 We note that an East Asian origin in warm temperate or tropical forests is
645 consistent with several other relevant lines of evidence developed in the study of *Viburnum*
646 evolution, biogeography, and ecology. Previous efforts to reconstruct the ancestral biome of
647 *Viburnum* have weakly favored warm temperate (Spriggs et al. 2015) or cold temperate
648 (Lens et al. 2016) conditions; neither study definitively supported or ruled out a cold
649 temperate origin. Similarly, Edwards et al. (2017) established a relationship between cold
650 temperate conditions and the evolution of deciduousness in *Viburnum*, but could not
651 resolve whether the MRCA was deciduous (cold-adapted) or evergreen (tropical or
652 warm-adapted). Landis et al. (2019) estimated a warm temperate origin of *Viburnum*, with
653 no support for a cold temperate origin, through a combined-evidence tip-dating analysis
654 (Ronquist et al. 2012) that included fossil pollen coded with biome characters to inform the
655 ancestral biome estimates. As a fossil-based estimate, the finding of a non-freezing origin of
656 *Viburnum* cannot be accepted unconditionally; the estimate depends crucially upon the
657 accuracy of biome state assignments to the fossil taxa, and also upon the spatial and
658 temporal biases inherent to fossil deposition and recovery. But, importantly, the
659 fossil-aware biome estimates of Landis et al. (2019) were obtained under the equivalent of
660 our *Null Biome* model, while the fossil-naive estimates in the present study were obtained
661 under the *Paleobiome* model. It is highly satisfying that both studies rule out a cold
662 temperate ancestry for *Viburnum*, and that they do so by leveraging alternative lines of
663 paleobiological evidence: the phylogenetic placement of fossils assigned to particular biomes
664 in one case, and the inferred spatial distribution of biomes through time in the other.

665 Examining only extant *Viburnum* species, the clade displays considerable variation

666 in both which biomes and which regions lineages occupy. Yet, each region does not contain
667 equal proportions of lineages with affinities to the three biomes. There are several possible
668 causes for this imbalance. In many cases, lineages may simply inhabit regions that lack
669 certain biomes; it is not surprising that there are no extant tropical lineages in North
670 America given that tropical forests have been marginal there since the Oligocene. In other
671 cases, lineages may not have had long enough periods of time for certain biome shifts. For
672 example, all Latin American lineages are adapted to warm temperate (cloud) forests, yet
673 none of them have adapted to the adjacent tropical forest biome. Given the young age of
674 the Latin American radiation, it is possible that there has not been enough time for them
675 to shift into the accessible tropical forests. In this case we can imagine that biological
676 factors (e.g., interactions with other species—competitors, herbivores, etc.—that have long
677 occupied tropical forests) may have played a significant role in limiting this shift
678 (Donoghue and Edwards 2014). In other cases, the imbalance may concern differential
679 rates of speciation or extinction within biomes. For instance, there are relatively few
680 tropical *Viburnum* species given the age and region of origin for the clade and given the
681 age of Asian tropical biomes. If tropical viburnums experienced increased extinction rates
682 (or decreased speciation rates) as they remained in an older biome, that effect would give
683 rise to a pattern of scattered, singular, distantly related, and anciently diverging tropical
684 lineages (“depauperons” of Donoghue and Sanderson 2015). This is precisely what we see
685 in the case of *V. clemensiae*, *V. amplificatum*, and *V. punctatum* (Spriggs et al. 2015).
686 From analyses under our simple *Paleobiome* model, it appears that temporal, geographical,
687 and ecological influences on rates of character evolution and lineage diversification may all
688 be important factors in explaining why *Viburnum* is distributed as it is across regions and
689 biomes.

690 Finally, although we question the general validity (often assumed) of “stepwise”
691 series of events (e.g., ‘trait-first’ versus ‘climate-first’ in the evolution of cold tolerance;
692 Edwards et al. 2015), we nevertheless explored how incorporating information on the past

693 distribution of biomes might influence the inference of biome-first versus region-first event
694 series. Specifically, we asked whether *Viburnum* lineages tended to shift biomes first or
695 disperse to a new region first when radiating through the mesic forests of Eurasia and the
696 New World. Taking the mean proportions across time intervals, we found that when
697 *Viburnum* lineages both disperse into new regions and shift into new biomes, region-first
698 event series (28% of series) are more common than biome-first (19%) series under the
699 *Paleobiome* model. Alone, this result is difficult to interpret, since the relative number and
700 size of biome and region states will influence what constitutes a biome shift or dispersal
701 event. Using the *Modern* analysis as a point of reference, we find a comparatively neutral
702 relationship, with roughly equal proportions of biome-first (20%) and region-first (21%)
703 series, while under the *Null Biome* analysis the *Paleobiome* relationship is inverted
704 (biome-first, 22%; region-first, 19%). When all regions contain all biomes (*Null Biome*), it
705 makes sense that the ratio of biome-first to region-first series is highest, and that it
706 decreases when the distribution of biomes is not uniform across regions (*Paleobiome* and
707 *Modern Biome*). In the case of *Viburnum*, it appears that several key regional shifts
708 between Eastern Asia and North America occurred a relatively long time ago, when
709 northern latitudes were still primarily covered by warm temperate forests (Fig. 8A). The
710 biome shifts into cold temperate forests occurred later, as cooling climates spread across
711 communities that were already assembled, which is compatible with the ‘lock-step’
712 hypothesis of (Edwards et al. 2017). Consistent with this scenario, we found that
713 region-first event series do not become the most common series type (over 35%) until the
714 Late Oligocene under the *Paleobiome* model (Fig. 8D). Such region-first event series have
715 also been inferred in several recent analyses, most notably by (Gagnon et al. 2019) who
716 found that *Caesalpinia* legumes moved frequently among succulent biomes on different
717 continents, and only later shifted into newly encountered biomes within each continent
718 (Donoghue 2019). From our findings, we suspect that ignoring paleobiome structure may
719 cause the number of region-first transition series to be underestimated. However, it must be

720 borne in our minds that our results may in part reflect the constraint built into our model
721 that simultaneous shifts in biome and region are not allowed (discussed below). In any case,
722 explicitly testing for the effect of paleobiome structure on event order will be important in
723 evaluating patterns of supposed phylogenetic biome conservatism (Crisp et al. 2009).

724 *Model discussion*

725 Although our model is simple, it is designed with certain statistical features that
726 would allow the model to be applied to diverse datasets beyond *Viburnum*, and to facilitate
727 extensions of the model towards more sophisticated designs. First, we treat many elements
728 in the evolutionary process as free parameters, whose values we estimate from the
729 phylogenetic dataset in question. For example, the w parameters control which layers of
730 the paleobiome graphical structure are most relevant to the evolutionary process, and the y
731 parameters control how dominant biomes (or regions) must be to receive dispersal or biome
732 shift events. Second, the Bayesian modeling framework we chose is ideal for managing
733 complex and parameter-rich hierarchical models (Höhna et al. 2016), allowing for future
734 models to explore the importance of other factors highlighted in the conceptual model of
735 Donoghue and Edwards (2014) — geographical distance (Webb and Ree 2012), region size
736 (Tagliacollo et al. 2015), biome size and shared perimeter (Cardillo et al. 2017), ecological
737 distance (Meseguer et al. 2015), and the effect of biotic interactions on trait and range
738 evolution (Quintero and Landis 2019) – by introducing new parameterizations for
739 computing the time-stratified rate matrices, $Q(m)$. Our Bayesian framework is also capable
740 of sources of uncertainty in the paleobiome graphs, such as uncertainty in the age of the
741 appearance of a biome within a region (Landis et al. 2018).

742 In our application of the model, we defined only three biomes and six regions,
743 but the general framework translates to other biogeographical systems with different
744 regions and biomes, provided one can construct an adequate time series of paleobiome
745 graphs. Though our literature-based approach to paleobiome graph construction was

746 somewhat subjective, we found it to be the most integrative way to summarize varied
747 global biome reconstructions, as most individual studies are purely qualitative (Wolfe 1985;
748 Morley 2000; Jetz and Fine 2012 Willis and McElwain 2014; Graham 2011; Graham 2018;
749 but see Kaplan et al. 2003) and based on disparate lines of paleoecological,
750 paleoclimatological, and paleogeological evidence. We believe that our paleobiome graphs
751 for the Northern Hemisphere are sufficiently accurate to show that spatial and temporal
752 variation in the distribution of tropical, warm temperate, and cold temperate forest biomes
753 in space and time can influence how species ranges and biome affinities evolve over time.
754 Nonetheless, future studies should explore more quantitative approaches to defining
755 paleobiome structures for use with the time-stratified regional biome shift model.

756 Our simple model of regional biome shifts lacks several desired features. Perhaps
757 most importantly, lineages in our model may only occupy a single region and a single
758 biome at a time. On paper, it is straightforward to extend the concepts of this model to
759 standard multi-character models, such as the Dispersal-Extinction-Cladogenesis model
760 (Ree et al. 2005; Matzke 2014; Sukumaran et al. 2015). As a DEC model variant, lineages
761 would be capable of gaining affinities with any biomes available within their range. For
762 example, for M biomes and N regions, there are on the order of 2^{M+N} combinations of
763 presences and absences across biomes and regions, and on the order of 2^{MN} combinations if
764 region-specific biome occupancies are considered. Computationally, this creates a vast
765 number of viable state combinations, many of which cannot be eliminated from the state
766 space (Webb and Ree 2012). Such a large state space will hinder standard likelihood-based
767 inference procedures for discrete biogeography (Ree and Sanmartín 2009), though recent
768 methodological advances addressing this problem should prove useful (Landis et al. 2013;
769 Quintero and Landis 2019).

770 Geographical state-dependent diversification (GeoSSE) models may also be
771 interfaced with our model. Incorporating the effect of biome availability on the extinction
772 rate would, at a minimum, be a very important contribution towards explaining patterns of

773 extant diversity. For example, tropical biomes have declined in dominance since the
774 Paleogene, and many ancient *Viburnum* lineages may have since gone extinct in the
775 tropics, perhaps owing to biotic interactions (the “dying embers” hypothesis of Spriggs
776 et al. 2015). In this sense, we expect that our model will overestimate how long a lineage
777 may persist in a region that lacks the appropriate biome, since our model does not threaten
778 ill-adapted species with higher extinction rates. Efforts to extend GeoSSE models in this
779 manner will face similar, if not more severe, challenges to those encountered in the DEC
780 framework, both in terms of computational limits and numbers of parameters (Beaulieu
781 and O’Meara 2016; Caetano et al. 2018).

782 If diversification rates vary conditionally on a lineage’s biome-region state, then so
783 should the underlying divergence time estimates. At a minimum, one should jointly
784 estimate divergence times and diversification dynamics to correctly propagate uncertainty
785 in phylogenetic estimates through to ancestral state estimates (Höhna et al. 2019). Beyond
786 that, paleogeographically structured models of biogeography have been shown to be useful
787 for estimating divergence times (Landis 2017; Landis et al. 2018). Paleoecological models,
788 such as our *Paleobiome* model, could be useful in some cases, perhaps for dating clades
789 where some degree of phylogenetic niche conservatism can be safely assumed (Wiens and
790 Donoghue 2004; Crisp et al. 2009; but see Donoghue and Edwards 2014 for potential
791 pitfalls with this approach). For instance, Baldwin and Sanderson (1998) hypothesized that
792 continental tarweeds (*Madiinae*, Asteraceae) radiated within the seasonally dry California
793 Floristic Province only after Miocene aridification created the province. Baldwin and
794 Sanderson translated this relationship between biome age and biome affinity to date the
795 maximum crown age of tarweeds, and thus date the maximum crown age of a notable
796 radiation nested within the tarweeds, the Hawaiian silversword alliance. In the future,
797 rather than calibrating the age of tarweeds by asserting a paleoecological hypothesis, it
798 would be possible to use our biome shift model to measure the probability of the “dry
799 radiation” scenario against competing scenarios, thereby dating the tarweeds (or other

800 clades) based on what ecological opportunities they made use of in different areas and at
801 different times (Baldwin and Sanderson 1998; Landis 2017; Landis et al. 2018).

802 Finally, although we have compared inferences of event series under several biome
803 structure models, and have argued that paleobiome models can influence such inferences,
804 we caution that event series themselves may not be accurate descriptors of some relevant
805 evolutionary scenarios. For example, it is entirely possible that a shift into a new biome
806 could occur during a transition from one region into another (e.g., adaptation to cold
807 forests during range expansion through Beringia, or the long-distance dispersal of an
808 organism already pre-adapted to occupy a novel biome). Such scenarios highlight that the
809 model we have presented here is simplistic in some of its basic assumptions. We view it as
810 a start in the right direction, and look forward to extensions that will allow us to test a
811 variety of more nuanced hypotheses.

812 CONCLUSION

813 The potential for a lineage to adapt to new biomes depends in part on the
814 geographical opportunities those lineages encountered in time and space. In the case of
815 *Viburnum*, we have shown that differing assumptions about the past distribution of biomes
816 can have a significant impact on ancestral biome estimates. And, when we integrate
817 information about the changing distribution of biomes through time, we favor an origin of
818 *Viburnum* in warm temperate or tropical forests, and confidently rule out an origin in cold
819 temperate forests. The confluence of this line of evidence with our analyses based instead
820 on fossil biome assignments (Landis et al. 2019) provides much greater confidence in a
821 result that orients our entire understanding of the direction of evolution and ecological
822 diversification in this clade.

823 More generally, we hope that our analyses will motivate biogeographers who wish to
824 estimate ancestral biomes to account for variation in the spatial distribution of biomes
825 through time. While we have achieved some conceptual understanding of the interplay

826 between biome shifts in lineages and biome distributions over time, many theoretical and
827 statistical problems must still be solved for us to fully appreciate the significance of
828 changing biome availability in generating Earth's biodiversity. In presenting our simple
829 model, we hope to provoke further inquiry into how life diversified throughout the biomes
830 of an ever-changing planet.

831 FUNDING

832 This work was supported by the NSF Postdoctoral Fellowship (DBI-1612153) to
833 MJL and a Gaylord Donnelley Environmental Fellowship to MJL through the Yale Institute
834 of Biospheric Studies. Our research on *Viburnum* has been funded through a series of NSF
835 awards to MJD and EJE (most recently, DEB-1557059 and DEB-1753504), and in part
836 through the Division of Botany of the Yale Peabody Museum of Natural History.

837 ACKNOWLEDGEMENTS

838 Ignacio Quintero, Nate Upham, David Polly, and Tracy Heath provided useful
839 feedback that helped us frame the context of the research. We also wish to thank Paul
840 Valdes, who provided us with various BIOME4 reconstructions. Finally, we express
841 gratitude to the Donoghue, Edwards, and Near lab groups for their helpful comments.

842 BIOSKETCHES

843 The authors are broadly interested in biodiversity, biogeography, and evolution in
844 plants. Author contributions: MJL, EJE, and MJD conceived the study. MJL designed the
845 model, executed the analyses, and produced the figures. MJL, EJE, and MJD interpreted
846 the results and wrote the manuscript. All authors reviewed the manuscript.

*

847

848 References

- 849 B. G. Baldwin and M. J. Sanderson. Age and rate of diversification of the Hawaiian
850 silversword alliance (Compositae). *Proceedings of the National Academy of Sciences*, 95
851 (16):9402–9406, 1998.
- 852 J. M. Beaulieu and B. C. O’Meara. Detecting hidden diversification shifts in models of
853 trait-dependent speciation and extinction. *Systematic Biology*, 65(4):583–601, 2016.
- 854 F. Bielejec, P. Lemey, G. Baele, A. Rambaut, and M. A. Suchard. Inferring heterogeneous
855 evolutionary processes through time: from sequence substitution to phylogeography.
856 *Systematic Biology*, 63:493–504, 2014.
- 857 S. Buerki, F. Forest, N. Alvarez, J. A. A. Nylander, N. Arrigo, and I. Sanmartín. An
858 evaluation of new parsimony-based versus parametric inference methods in biogeography:
859 a case study using the globally distributed plant family Sapindaceae. *Journal of
860 Biogeography*, 38:531–550, 2011.
- 861 D. S. Caetano, B. C. O’Meara, and J. M. Beaulieu. Hidden state models improve
862 state-dependent diversification approaches, including biogeographical models. *Evolution*,
863 72(11):2308–2324, 2018.
- 864 M. Cardillo, P. H. Weston, Z. K. M. Reynolds, P. M. Olde, A. R. Mast, E. M. Lemmon,
865 A. R. Lemmon, and L. Bromham. The phylogeny and biogeography of *Hakea*
866 (Proteaceae) reveals the role of biome shifts in a continental plant radiation. *Evolution*,
867 71(8):1928–1943, 2017.
- 868 D. S. Chatelet, W. L. Clement, L. Sack, M. J. Donoghue, and E. J. Edwards. The
869 evolution of photosynthetic anatomy in *Viburnum* (Adoxaceae). *International Journal of
870 Plant Sciences*, 174(9):1277–1291, 2013.

- 871 W. L. Clement, M. Arakaki, P. W. Sweeney, E. J. Edwards, and M. J. Donoghue. A
872 chloroplast tree for *Viburnum* (Adoxaceae) and its implications for phylogenetic
873 classification and character evolution. *American Journal of Botany*, 101(6):1029–1049,
874 2014.
- 875 M. D. Crisp, M. T. K. Arroyo, L. G. Cook, M. A. Gandolfo, G. J. Jordan, M. S. McGlone,
876 P. H. Weston, M. Westoby, P. Wilf, and P. H. Linder. Phylogenetic biome conservatism
877 on a global scale. *Nature*, 458(7239):754–756, 2009.
- 878 M. J. Donoghue. A phylogenetic perspective on the distribution of plant diversity.
879 *Proceedings of the National Academy of Sciences*, 105:11549–11555, 2008.
- 880 M. J. Donoghue. Adaptation meets dispersal: legumes in the land of succulents. *New
881 Phytologist*, 222:1667–1669, 2019.
- 882 M. J. Donoghue and E. J. Edwards. Biome shifts and niche evolution in plants. *Annual
883 Review of Ecology, Evolution, and Systematics*, 45:547–572, 2014.
- 884 M. J. Donoghue and M. J. Sanderson. Confluence, synnovation, and depauperons in plant
885 diversification. *New Phytologist*, 207(2):260–274, 2015.
- 886 D. A. R. Eaton, E. L. Spriggs, B. Park, and M. J. Donoghue. Misconceptions on missing
887 data in RAD-seq phylogenetics with a deep-scale example from flowering plants.
888 *Systematic Biology*, 66(3):399–412, 2017.
- 889 E. J. Edwards, J. M. de Vos, and M. J. Donoghue. Doubtful pathways to cold tolerance in
890 plants. *Nature*, 521(7552):E5, 2015.
- 891 E. J. Edwards, D. S. Chatelet, B. Chen, J. Y. Ong, S. Tagane, H. Kanemitsu, K. Tagawa,
892 K. Teramoto, B. Park, K. Chung, J. Hu, T. Yahara, and M. J. Donoghue. Convergence,
893 consilience, and the evolution of temperate deciduous forests. *The American Naturalist*,
894 190(S1):S87–S104, 2017.

- 895 J. Felsenstein. Evolutionary trees from DNA sequences: A maximum likelihood approach.
896 *Journal of Molecular Evolution*, 17:368–376, 1981.
- 897 P. V. A. Fine and R. H. Ree. Evidence for a time-integrated species-area effect on the
898 latitudinal gradient in tree diversity. *The American Naturalist*, 168(6):796–804, 2006.
- 899 E. Gagnon, J. J. Ringelberg, A. Bruneau, G. P. Lewis, and C. E. Hughes. Global Succulent
900 Biome phylogenetic conservatism across the pantropical Caesalpinia Group
901 (Leguminosae). *New Phytologist*, 222:1994–2008, 2019.
- 902 E. E. Goldberg, K. Roy, R. Lande, and D. Jablonski. Diversity, endemism, and age
903 distributions in macroevolutionary sources and sinks. *The American Naturalist*, 165(6):
904 623–633, 2005.
- 905 A. Graham. *A natural history of the New World: the ecology and evolution of plants in the
906 Americas*. University of Chicago Press, 2011.
- 907 A. Graham. *Land Bridges Ancient Environments, Plant Migrations, and New World
908 Connections*. University of Chicago Press, 2018.
- 909 T. A. Heath, J. P. Huelsenbeck, and T. Stadler. The fossilized birth–death process for
910 coherent calibration of divergence-time estimates. *Proceedings of the National Academy
911 of Sciences*, 111(29):E2957–E2966, 2014.
- 912 N. Herold, J. Buzan, M. Seton, A. Goldner, J. A. M. Green, R. D. Müller, P. Markwick,
913 and M. Huber. A suite of early Eocene (~55 Ma) climate model boundary conditions.
914 *Geoscientific Model Development*, 7(5):2077–2090, 2014.
- 915 S. Höhna, M. J. Landis, T. A. Heath, B. Boussau, N. Lartillot, B. R. Moore, J. P.
916 Huelsenbeck, and F. Ronquist. RevBayes: Bayesian phylogenetic inference using
917 graphical models and interactive model-specification language. *Systematic Biology*, 65:
918 726–736, 2016.

- 919 S. Höhna, W. A. Freyman, Z. Nolen, J. P. Huelsenbeck, M. R. May, and B. R. Moore. A
920 Bayesian Approach for Estimating Branch-Specific Speciation and Extinction Rates.
921 *bioRxiv*, 2019. doi: 10.1101/555805.
- 922 H. Jeffreys. *Theory of Probability*. Oxford University Press, Oxford, 1961.
- 923 W. Jetz and P. V. A. Fine. Global gradients in vertebrate diversity predicted by historical
924 area-productivity dynamics and contemporary environment. *PLoS Biology*, 10(3):
925 e1001292, 2012.
- 926 J. O. Kaplan, N. H. Bigelow, I. C. Prentice, S. P. Harrison, P. J. Bartlein, T. R.
927 Christensen, W. Cramer, N. V. Matveyeva, D. A. McGuire, D. F. Murray, and V. Y.
928 Razzhivin. Climate change and Arctic ecosystems: 2. Modeling, paleodata-model
929 comparisons, and future projections. *Journal of Geophysical Research: Atmospheres*, 108
930 (D19), 2003.
- 931 K. V. Klaus and N. J. Matzke. Statistical comparison of trait-dependent biogeographical
932 models indicates that podocarpaceae dispersal is influenced by both seed cone traits and
933 geographical distance. *Systematic Biology*, 2019.
- 934 M. J. Landis. Biogeographic dating of speciation times using paleogeographically informed
935 processes. *Systematic Biology*, 66(23):128–144, 2017.
- 936 M. J. Landis, N. J. Matzke, B. R. Moore, and J. P. Huelsenbeck. Bayesian analysis of
937 biogeography when the number of areas is large. *Systematic Biology*, 62:789–804, 2013.
- 938 M. J. Landis, W. A. Freyman, and B. G. Baldwin. Retracing the Hawaiian silversword
939 radiation despite phylogenetic, biogeographic, and paleogeographic uncertainty.
940 *Evolution*, 72(11):2343–2359, 2018.
- 941 M. J. Landis, D. A. R. Eaton, W. L. Clement, B. Park, E. L. Spriggs, P. W. Sweeney, E. J.
942 Edwards, and M. J. Donoghue. Joint phylogenetic estimation of geographic movements

- 943 and biome shifts during the global diversification of *Viburnum*. *bioRxiv*, 2019. doi:
944 10.1101/811067.
- 945 R. E. Latham and R. E. Ricklefs. Continental comparisons of temperate-zone tree species
946 diversity. *Species diversity in ecological communities: historical and geographical*
947 *perspectives*, pages 294–314, 1993.
- 948 F. Lens, R. A. Vos, G. Charrier, T. van der Niet, V. Merckx, P. Baas, J. Aguirre Gutierrez,
949 B. Jacobs, L. Chacon Dória, E. Smets, and S. Delzon. Scalariform-to-simple transition in
950 vessel perforation plates triggered by differences in climate during the evolution of
951 Adoxaceae. *Annals of Botany*, 118(5):1043–1056, 2016.
- 952 L. Lu, P. W. Fritsch, N. J. Matzke, H. Wang, K. A. Kron, D. Z. Li, and J. J. Wiens. Why
953 is fruit colour so variable? phylogenetic analyses reveal relationships between fruit-colour
954 evolution, biogeography and diversification. *Global Ecology and Biogeography*, 28(7):
955 891–903, 2019.
- 956 P. Matos-Maraví, N. J. Matzke, F. J. Larabee, R. M. Clouse, W. C. Wheeler, D. M. Sorger,
957 A. V. Suarez, and M. Janda. Taxon cycle predictions supported by model-based
958 inference in Indo-Pacific trap-jaw ants (Hymenoptera: Formicidae: *Odontomachus*).
959 *Molecular Ecology*, 27(20):4090–4107, 2018.
- 960 N. J. Matzke. Model selection in historical biogeography reveals that founder-event
961 speciation is a crucial process in island clades. *Systematic Biology*, 63:951–970, 2014.
- 962 A. S. Meseguer, J. M. Lobo, R. Ree, D. J. Beerling, and I. Sanmartín. Integrating Fossils,
963 Phylogenies, and Niche Models into Biogeography to Reveal Ancient Evolutionary
964 History: The Case of *Hypericum* (Hypericaceae). *Systematic Biology*, 64(2):215–232,
965 2015.
- 966 R. J. Morley. *Origin and evolution of tropical rain forests*. John Wiley & Sons, 2000.

- 967 L. Mucina. Biome: evolution of a crucial ecological and biogeographical concept. *New
968 Phytologist*, 222:97–114, 2019.
- 969 D. M. Olson, E. Dinerstein, E. D. Wikramanayake, N. D. Burgess, G. V. N. Powell, E. C.
970 Underwood, J. A. D'amico, I. Itoua, H. E. Strand, J. C. Morrison, et al. Terrestrial
971 ecoregions of the world: A new map of life on earth a new global map of terrestrial
972 ecoregions provides an innovative tool for conserving biodiversity. *BioScience*, 51(11):
973 933–938, 2001.
- 974 M. Pagel. Detecting correlated evolution on phylogenies: a general method for the
975 comparative analysis of discrete characters. *Proceedings of the Royal Society of London.
976 Series B: Biological Sciences*, 255(1342):37–45, 1994.
- 977 M. J. Pound and U. Salzmann. Heterogeneity in global vegetation and terrestrial climate
978 change during the Late Eocene to Early Oligocene transition. *Scientific Reports*, 7:43386,
979 2017.
- 980 M. J. Pound, A. M. Haywood, U. Salzmann, J. B. Riding, D. J. Lunt, and S. J. Hunter. A
981 Tortonian (Late Miocene, 11.61 - 7.25 Ma) global vegetation reconstruction.
982 *Palaeogeography, Palaeoclimatology, Palaeoecology*, 300(1-4):29–45, 2011.
- 983 M. J. Pound, A. M. Haywood, U. Salzmann, and J. B. Riding. Global vegetation dynamics
984 and latitudinal temperature gradients during the Mid to Late Miocene (15.97 – 5.33
985 Ma). *Earth Science Reviews*, 112(1-2):1–22, 2012.
- 986 I. C. Prentice, W. Cramer, S. P. Harrison, R. Leemans, R. A. Monserud, and A. M.
987 Solomon. A global biome model based on plant physiology and dominance, soil
988 properties and climate. *Journal of Biogeography*, pages 117–134, 1992.
- 989 I. Quintero and M. J. Landis. Interdependent Phenotypic and Biogeographic Evolution
990 Driven by Biotic Interactions. *bioRxiv*, 2019. doi: 10.1101/560912.

- 991 R. H. Ree and I. Sanmartín. Prospects and challenges for parametric models in historical
992 biogeographical inference. *Journal of Biogeography*, 36:1211–1220, 2009.
- 993 R. H. Ree and S. A. Smith. Maximum likelihood inference of geographic range evolution by
994 dispersal, local extinction, and cladogenesis. *Systematic Biology*, 57:4–14, 2008.
- 995 R. H. Ree, B. R. Moore, C. O. Webb, and M. J. Donoghue. A likelihood framework for
996 inferring the evolution of geographic range on phylogenetic trees. *Evolution*, 59:
997 2299–2311, 2005.
- 998 F. Ronquist, S. Klopfstein, L. Vilhelmsen, S. Schulmeister, D. L. Murray, and A. P.
999 Rasnitsyn. A total-evidence approach to dating with fossils, applied to the early
1000 radiation of the Hymenoptera. *Systematic Biology*, 61(6):973–999, 2012.
- 1001 U. Salzmann, A. M. Haywood, D. J. Lunt, P. J. Valdes, and D. J. Hill. A new global biome
1002 reconstruction and data-model comparison for the Middle Pliocene. *Global Ecology and*
1003 *Biogeography*, 17(3):432–447, 2008.
- 1004 U. Salzmann, A. M. Haywood, and D. J. Lunt. The past is a guide to the future?
1005 Comparing Middle Pliocene vegetation with predicted biome distributions for the
1006 twenty-first century. *Philosophical Transactions: Series A: Mathematical, physical, and*
1007 *engineering sciences*, 367(1886):189–204, 2009.
- 1008 S. B. Schmerler, W. L. Clement, J. M. Beaulieu, D. S. Chatelet, L. Sack, M. J. Donoghue,
1009 and E. J. Edwards. Evolution of leaf form correlates with tropical–temperate transitions
1010 in *Viburnum* (Adoxaceae). *Proceedings of the Royal Society B: Biological Sciences*, 279
1011 (1744):3905–3913, 2012.
- 1012 C. Scoffoni, D. S. Chatelet, J. Pasquet-Kok, M. Rawls, M. J. Donoghue, E. J. Edwards,
1013 and L. Sack. Hydraulic basis for the evolution of photosynthetic productivity. *Nature*
1014 *Plants*, 2(6):16072, 2016.

- 1015 E. L. Spriggs, W. L. Clement, P. W. Sweeney, S. Madriñán, E. J. Edwards, and M. J.
1016 Donoghue. Temperate radiations and dying embers of a tropical past: the diversification
1017 of viburnum. *New Phytologist*, 207:340–354, 2015.
- 1018 J. Sukumaran and L. L. Knowles. Trait-dependent biogeography:(re) integrating biology
1019 into probabilistic historical biogeographical models. *Trends in Ecology & Evolution*, 33:
1020 390–398, 2018.
- 1021 J. Sukumaran, E. P. Economo, and L. L. Knowles. Machine learning biogeographic
1022 processes from biotic patterns: A new trait-dependent dispersal and diversification
1023 model with model choice by simulation-trained discriminant analysis. *Systematic
1024 Biology*, page syv121, 2015.
- 1025 V. A. Tagliacollo, S. M. Duke-Sylvester, W. A. Matamoros, P. Chakrabarty, and J. S.
1026 Albert. Coordinated dispersal and pre-Isthmian assembly of the Central American
1027 ichthyofauna. *Systematic Biology*, 66:183–196, 2015.
- 1028 I. Verdinelli and L. Wasserman. Computing Bayes factors using a generalization of the
1029 Savage-Dickey density ratio. *Journal of the American Statistical Association*, 90:614–618,
1030 1995.
- 1031 C. O. Webb and R. H. Ree. Historical biogeography inference in Malesia. In D. Gower,
1032 K. Johnson, J. Richardson, B. Rosen, L. Ruber, and S. Williams, editors, *Biotic
1033 evolution and environmental change in Southeast Asia*, pages 191–215. Cambridge
1034 University Press, 2012.
- 1035 A. Weeks, F. Zapata, S. K. Pell, D. C. Daly, J. D. Mitchell, and P. V. A. Fine. To move or
1036 to evolve: contrasting patterns of intercontinental connectivity and climatic niche
1037 evolution in “Terebinthaceae” (Anacardiaceae and Burseraceae). *Frontiers in Genetics*,
1038 5:409, 2014. doi: 10.3389/fgene.2014.00409.
- 1039 R. H. Whittaker. *Communities and Ecosystems*. Macmillan Company, 1970.

- 1040 H. Wickham. *ggplot2: elegant graphics for data analysis*. Springer, 2016.
- 1041 J. J. Wiens and M. J. Donoghue. Historical biogeography, ecology and species richness.
- 1042 *Trends in Ecology & Evolution*, 19(12):639–644, 2004.
- 1043 K. Willis and J. McElwain. *The evolution of plants*. Oxford University Press, 2014.
- 1044 J. A. Wolfe. Distribution of major vegetational types during the tertiary. *The carbon cycle and atmospheric CO₂: natural variations Archean to present*, 32:357–375, 1985.
- 1045